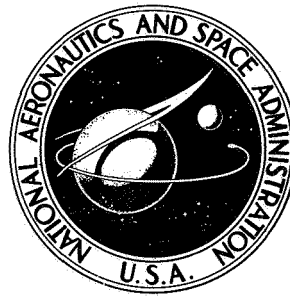


NASA TECHNICAL NOTE



NASA TN D-7228

NASA TN D-7228

**A METHOD FOR ESTIMATING STATIC
AERODYNAMIC CHARACTERISTICS FOR
SLENDER BODIES OF CIRCULAR AND
NONCIRCULAR CROSS SECTION ALONE
AND WITH LIFTING SURFACES AT
ANGLES OF ATTACK FROM 0° TO 90°**

by Leland H. Jorgensen

Ames Research Center

Moffett Field, Calif. 94035

NATIONAL AERONAUTICS AND SPACE ADMINISTRATION • WASHINGTON, D. C. • APRIL 1973

1. Report No. NASA TN D-7228	2. Government Accession No.	3. Recipient's Catalog No.	
4. Title and Subtitle A METHOD FOR ESTIMATING STATIC AERODYNAMIC CHARACTERISTICS FOR SLENDER BODIES OF CIRCULAR AND NONCIRCULAR CROSS SECTION ALONE AND WITH LIFTING SURFACES AT ANGLES OF ATTACK FROM 0° TO 90°		5. Report Date April 1973	
		6. Performing Organization Code	
7. Author(s) Leland H. Jorgensen		8. Performing Organization Report No. A-4700	
		10. Work Unit No. 501-06-05-00-21	
9. Performing Organization Name and Address NASA-Ames Research Center Moffett Field, Calif. 94035		11. Contract or Grant No.	
		13. Type of Report and Period Covered Technical Note	
12. Sponsoring Agency Name and Address National Aeronautics and Space Administration Washington, D. C., 20546		14. Sponsoring Agency Code	
		15. Supplementary Notes	
16. Abstract <p>An engineering-type method is presented for estimating normal-force, axial-force, and pitching-moment coefficients for slender bodies of circular and noncircular cross section alone and with lifting surfaces. Static aerodynamic characteristics computed by the method are shown to agree closely with experimental results for slender bodies of circular and elliptic cross section and for winged-circular and winged-elliptic cones. However, the present experimental results used for comparison with the method are limited to angles of attack only up to about 20° and Mach numbers from 2 to 4.</p>			
17. Key Words (Suggested by Author(s)) Body theory Noncircular body theory Wing-body theory High angles of attack		18. Distribution Statement Unclassified - Unlimited	
19. Security Classif. (of this report) Unclassified	20. Security Classif. (of this page) Unclassified	21. No. of Pages 39	22. Price* \$3.00

TABLE OF CONTENTS

	<u>Page</u>
NOTATION	v
SUMMARY	1
INTRODUCTION	1
PROCEDURE AND FORMULAS FOR COMPUTING AERODYNAMIC CHARACTERISTICS	2
Body Alone Method of Reference 9	3
General Case for a Body Alone or With Lifting Surfaces	5
Special Case for an Elliptic Cone With Triangular Wing	6
Formulas and Values of $(C_n/C_{n_0})_{SB}$ and $(C_n/C_{n_0})_{Newt}$ for Winged-Elliptic Cross Sections	7
$(C_n/C_{n_0})_{SB}$ formulas	7
$(C_n/C_{n_0})_{Newt}$ formulas	9
Values of $(C_n/C_{n_0})_{SB}$ and $(C_n/C_{n_0})_{Newt}$	9
COMPARISON OF COMPUTED WITH EXPERIMENTAL AERODYNAMIC CHARACTERISTICS	10
Models Studied and Test Conditions	10
Bodies with circular and elliptic cross sections	10
Winged-circular and winged-elliptic cones	10
Computation of Aerodynamic Characteristics	11
Comparison of Computed With Experimental Characteristics for Bodies With Circular and Elliptic Cross Sections	11
Comparison of Computed With Experimental Characteristics for Winged-Circular and Winged-Elliptic Cones	12
CONCLUDING REMARKS	13
REFERENCES	14
FIGURES	17

NOTATION

A	body cross-sectional area
A_b	body base area (at $x = \ell$)
A_p	planform area
A_r	reference area (taken as A_b for the comparisons of computed with experimental results)
a, b	semimajor and semiminor axes of elliptic cross section
C_A	axial-force coefficient, $\frac{F_a}{q_\infty A_r}$
C_{d_n}	crossflow drag coefficient of circular cylinder section, $\frac{F_n}{q_n(\Delta \ell_{cy})d_{cy}}$
C_D	drag coefficient, $\frac{\text{drag}}{q_\infty A_r}$
C_L	lift coefficient, $\frac{\text{lift}}{q_\infty A_r}$
C_m	pitching-moment coefficient about station at x_m from nose, $\frac{\text{pitching moment}}{q_\infty A_r X}$
C_N	normal-force coefficient, $\frac{F_n}{q_\infty A_r}$
C_n	local normal-force coefficient per unit length
C_p	pressure coefficient, $\frac{p - p_\infty}{q_\infty}$
d	body cross-section diameter
F_a, F_n	axial and normal forces
ℓ	body length
M_n	Mach number component normal to body axis, $M_\infty \sin \alpha$
M_∞	free-stream Mach number
p	pressure
p_∞	free-stream static pressure
q_n	dynamic pressure component normal to body axis, $q_\infty \sin^2 \alpha$
q_∞	free-stream dynamic pressure, $\frac{1}{2} \rho V_\infty^2$

r	body cross-section radius
s	semispan
Re	free-stream Reynolds number, $\frac{\rho V_{\infty} X}{\mu}$
Re_n	Reynolds number component normal to body axis, $Re \frac{d}{X} \sin \alpha$
V	body volume
V_n	velocity component normal to body axis, $V_{\infty} \sin \alpha$
V_{∞}	free-stream velocity
w	body width
X	reference length
x	axial distance from body nose
x_{ac}	distance from nose to aerodynamic force center
x_c	distance from nose to centroid of body planform area
x_m	distance from nose to pitching-moment reference center
α	angle of attack
β	$\sqrt{M_{\infty}^2 - 1}$
ϵ	wing planform semiapex angle
η	crossflow drag proportionality factor
τ	ratio of the lift of a triangular wing by linearized theory to the lift by slender-body theory
μ	viscosity coefficient of air
ρ	density of air
φ	angle of bank about body longitudinal axis

Subscripts

cy	cylinder
$Newt$	Newtonian theory
vi	

o equivalent circular body or cross section

SB slender-body theory

stag stagnation

**A METHOD FOR ESTIMATING STATIC AERODYNAMIC CHARACTERISTICS FOR
SLENDER BODIES OF CIRCULAR AND NONCIRCULAR CROSS SECTION
ALONE AND WITH LIFTING SURFACES AT ANGLES OF ATTACK
FROM 0° TO 90°**

Leland H. Jorgensen

Ames Research Center

SUMMARY

An engineering-type method is presented for estimating normal-force, axial-force, and pitching-moment coefficients for slender bodies of circular and noncircular cross section alone and with lifting surfaces. In the generalized equations that are given for C_N and C_m , ratios are required of the local normal-force coefficient per unit length for the cross section of interest to that for the equivalent circular cross section. These ratios are given both from slender-body and Newtonian theories. Formulas and numerical values of these ratios for winged-elliptic cross sections are included in the report.

Static aerodynamic characteristics computed by the method are shown to agree closely with experimental results for slender bodies of circular and elliptic cross section and for winged-circular and winged-elliptic cones. However, because the experimental results are limited to angles of attack of less than about 20° and Mach numbers only from 2 to 4, further comparison of the method with more data is needed to determine validity limits for the method. The method may be applicable or adaptable for use at subsonic, supersonic, and low hypersonic Mach numbers.

INTRODUCTION

High angle-of-attack aerodynamics is increasing in importance because of the demand for greater maneuverability of space shuttle vehicles, missiles, and military aircraft (both manned and remotely piloted). At present there appears to be a lack of analytical methods and aerodynamic data applicable to the design of advanced configurations for flight at high angles of attack over a wide range of Mach and Reynolds numbers.

The purpose of this report is to present an engineering-type method for estimating the normal-force, axial-force, and pitching-moment coefficients for slender bodies of circular and noncircular cross section alone and with lifting surfaces (such as wings and tails) at angles of attack from 0° to 90°. Effects of body and wing vortex flows on tail surfaces and controls are not included, and a complete analysis of wing-body-tail aerodynamics and control effectiveness is not pursued.

The method may be applicable or adaptable for use at subsonic, supersonic, and low hypersonic Mach numbers, although its true limits of applicability must await experimental verification. In the present report, computed force and moment characteristics are compared with available experimental

results for bodies of circular and elliptic cross section and for winged-circular and winged-elliptic cones at angles of attack from 0° to about 20° and Mach numbers from about 2 to 4.

PROCEDURE AND FORMULAS FOR COMPUTING AERODYNAMIC CHARACTERISTICS

Prior to the work of Allen in 1949-51 (refs. 1 and 2) most analytical procedures for computing the aerodynamic characteristics of bodies and wing-body combinations were based on potential theory and were limited in usefulness to very low angles of attack. Allen proposed a method for predicting the static longitudinal forces and moments for bodies of revolution inclined to angles of attack considerably higher than those for which theories based only on potential-flow concepts are known to apply. In this method a crossflow lift attributed to flow separation is added to the lift predicted by potential theory. This method has been used quite successfully in computing the aerodynamic coefficients of inclined bodies (e.g., refs. 1-6), although most data available for study until 1961 were for bodies at angles of attack below about 20° , and the formulas were initially written to apply only over about this angle-of-attack range.

In 1961, Allen's concept (ref. 7) was adopted for computing the normal-force, axial-force, and pitching-moment coefficients for a rocket booster throughout the angle of attack range from 0° to 180° . Satisfactory agreement of theory with experiment was obtained for a test model of the rocket booster over the Mach number range from 0.6 to 4. Further application of the Allen concept was made by Saffell, Howard, and Brooks (ref. 8) in 1971 in a programmed method for predicting the static longitudinal aerodynamic characteristics of low aspect-ratio missiles operating at angles of attack up to 180° .

In 1958, a method for computing the aerodynamic characteristics for bodies of noncircular cross section was proposed (ref. 6). In this method, normal-force and pitching-moment coefficients (C_{N_0} and C_{m_0}) are computed by Allen's formulas for the equivalent body of revolution which has the same axial distribution of cross-sectional area as the noncircular body. Then the values of C_N and C_m for the noncircular body are computed from C_N/C_{N_0} and C_m/C_{m_0} ratios determined from apparent mass coefficients (i.e., from slender-body theory). Good agreement of theory with experiment (ref. 6) was obtained by this procedure for bodies of elliptic cross section at the conditions investigated (a/b 's from 1 to 2, φ 's of 0° and 90° , M_∞ 's from 2 to 4, and α 's from 0° to 20°).

Recently, in 1972, the Allen concept again has been applied in the development of an engineering-type procedure (ref. 9) for computing normal-force, axial-force, and pitching-moment coefficients for slender bodies of circular and noncircular cross sections at angle of attacks from 0° to 180° . The C_N and C_m formulas are written, however, for a body whose cross-sectional shape remains constant over the body length, but the cross-sectional area, of course, is allowed to vary.

In this section of the present report, the method of reference 9 is first reviewed. Then C_N and C_m expressions are written for the general case of a body alone or with lifting surfaces (e.g., wings) where the cross-sectional shape, as well as the cross-sectional area, is allowed to vary along the body length. For the special case of winged-elliptic cones, simplified expressions for C_N and C_m are also presented.

In all of these expressions for C_N and C_m , it is necessary to have values of local normal-force coefficient per unit length for the noncircular cross sections (C_n) ratioed to those for the equivalent circular body cross sections (C_{n_0}). Formulas for computing C_n/C_{n_0} ratios for winged-elliptic cross sections are given, and computed values for some typical cases are presented.

Body Alone Method of Reference 9

For a slender body whose cross-sectional shape is constant over its length, Jorgensen (ref. 9) has suggested equations for computing the normal-force, axial-force, and pitching-moment coefficients. For the sign convention in sketch (a) and for α 's from 0° to 90° , these equations are

$$C_N = \frac{A_b}{A_r} \sin 2\alpha \cos \frac{\alpha}{2} \left(\frac{C_N}{C_{N_0}} \right)_{SB} + \eta C_{d_n} \frac{A_p}{A_r} \sin^2 \alpha \left(\frac{C_N}{C_{N_0}} \right)_{Newt} \quad (1)$$

$$C_A = C_{A_{\alpha=0}} \cos^2 \alpha \quad (2)$$

and

$$C_m = \left\{ \left[\frac{V - A_b(\ell - x_m)}{A_r X} \right] \sin 2\alpha \cos \frac{\alpha}{2} \right\} \left(\frac{C_m}{C_{m_0}} \right)_{SB} + \left[\eta C_{d_n} \frac{A_p}{A_r} \left(\frac{x_m - x_c}{X} \right) \sin^2 \alpha \right] \left(\frac{C_m}{C_{m_0}} \right)_{Newt} \quad (3)$$

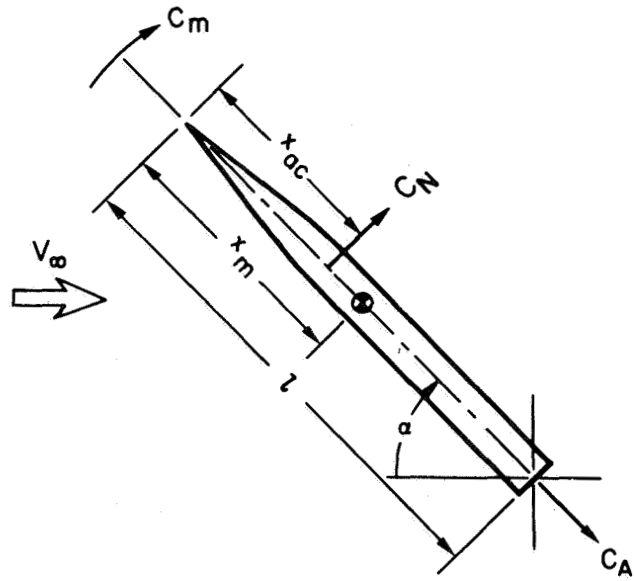
The aerodynamic force center is then given by

$$x_{ac} = \left(\frac{x_m}{X} - \frac{C_m}{C_N} \right) X \quad (4)$$

where X is the reference length.

The first terms in equations (1) and (3) come from slender-body potential theory. The second terms represent the viscous crossflow or crossflow attributed to flow separation.

In equation (1), (C_N/C_{N_0}) is the ratio of the normal-force coefficient for the body of noncircular cross section to that for the equivalent body of circular cross section (i.e., the circular body having the same area distribution). The ratio $(C_N/C_{N_0})_{SB}$ is determined from slender-body theory, and the ratio $(C_N/C_{N_0})_{Newt}$ is determined from Newtonian impact theory. For a body whose cross-



Sketch (a)

sectional shape is constant over its length, these ratios are equal to the ratios of the normal-force coefficients per unit length; that is,

$$\left(\frac{C_N}{C_{N_o}}\right)_{\text{SB}} = \left(\frac{C_m}{C_{m_o}}\right)_{\text{SB}} = \left(\frac{C_n}{C_{n_o}}\right)_{\text{SB}}$$

and

$$\left(\frac{C_N}{C_{N_o}}\right)_{\text{Newt}} = \left(\frac{C_m}{C_{m_o}}\right)_{\text{Newt}} = \left(\frac{C_n}{C_{n_o}}\right)_{\text{Newt}}$$

In equations (1) and (3), C_{d_n} is the crossflow drag coefficient for a section of an “infinite length” or truly two-dimensional circular cylinder placed normal to an airstream. It is a function of both the Mach number and Reynolds number components that are normal to the cylinder longitudinal axis, and hence for a body at angle of attack it is a function of

$$M_n = M_\infty \sin \alpha \quad (5)$$

and

$$Re_n = Re \sin \alpha \quad (6)$$

M_n is commonly called the crossflow Mach number and Re_n the crossflow Reynolds number. Necessary “state-of-the-knowledge” plots of C_{d_n} versus M_n and Re_n are given in reference 9.

The crossflow drag proportionality factor is η , that is, the ratio of the crossflow drag coefficient for a finite length cylinder to that for an infinite length cylinder. In reference 9, η 's from reference 10 are plotted as a function of length-to-width ratio for both circular cylinders and flat plates. It is suggested in reference 9 that η 's for noncircular as well as for circular bodies be estimated from this plot for bodies at subsonic free-stream Mach numbers. Because the curves for the circular cylinders and flat plates lie close together, estimates for noncircular bodies are easy to make. For bodies at supersonic and hypersonic free-stream Mach numbers, experience to date has shown that it is best to assume that $\eta = 1$ (ref. 9).

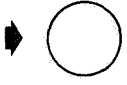
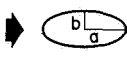
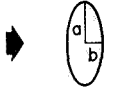
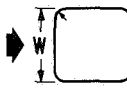
In the method of reference 9, C_N and C_m are controlled through C_{d_n} by either crossflow Mach number M_n or crossflow Reynolds number Re_n . Equations (1) and (3) have been written for the case of C_N and C_m controlled by M_n . It might be instructive to emphasize that there is some basic experimental justification, even at low subsonic M_n , for the use of Newtonian theory to determine the ratio C_N/C_{N_o} ($= C_n/C_{n_o}$) in the second term of equation (1). For various rounded and blunt two-dimensional cylinders (table 1), values of C_{d_n} and C_n/C_{n_o} computed by Newtonian and modified Newtonian theories agree reasonably well with measured results for subcritical values of M_n and Re_n . This agreement is shown in table 1 for the circular, elliptical, and square cross-sectional shapes considered.

For bodies at low subsonic M_n 's (below critical), the variation of C_{d_n} with Re_n for the cross section of interest can become significantly large as Re_n exceeds the critical value. For this Re_n controlled condition, equations (1) and (3) can be used with slight modification to the second

terms. $(C_N/C_{N_0})_{Newt}$ and $(C_m/C_{m_0})_{Newt}$ are removed, and experimental values of C_{d_n} are used for the cross section of interest. Note, however, that most experimental values of C_{d_n} are based on cross-sectional width w and must be multiplied by w/d , where d is the equivalent diameter of the cross section. In reference 9 a compilation of references is given from which experimental values of C_{d_n} vs Re_n can be obtained for various designated cross sections and flow directions.

The reader is referred to reference 9 for review of equations and methods for computing wave, skin-friction, and base-pressure contributions to C_A and for a method other than equation (2) for computing C_A .

TABLE 1.— C_{d_n} AND C_n/C_{n_0} VALUES FOR TWO-DIMENSIONAL CYLINDERS OF VARIOUS CROSS SECTIONS AT $\alpha = 90^\circ$ AS COMPUTED BY NEWTONIAN THEORIES AND MEASURED AT SUBCRITICAL MACH AND REYNOLDS NUMBERS

CROSS SECTION	NEWTONIAN THEORY		MOD. NEWT. THEORY FOR $C_{p_{stag}} = 1.8$		MEASURED			
	C_{d_n}	C_n/C_{n_0}	C_{d_n}	C_n/C_{n_0}	C_{d_n}	C_n/C_{n_0}	REF.	
	1.33	1.00	1.20	1.00	1.20	1.00	11	
 $a/b = 2$ $a/b = 4$	0.94	0.50	0.85	0.50	0.70	0.41	12, 13	
	0.59	0.22	0.53	0.22	0.35	0.15	12	
 $a/b = 2$	1.65	1.75	1.49	1.75	1.60	1.89	13, 14	
 $r = kw$	$k = 0.0$	2.00	1.33	1.80	1.33	2.05	1.51	12
	$k = 0.02$	1.97	1.33	1.78	1.33	2.00	1.48	13
	$k = 0.08$	1.89	1.26	1.70	1.26	1.65	1.22	15
	$k = 0.24$	1.68	1.14	1.51	1.14	1.12	0.85	15
	$k = 0.50$	1.33	1.00	1.20	1.00	1.20	1.00	11

NOTE: ALL C_{d_n} 's IN TABLE ARE BASED ON WIDTH OF CROSS SECTION, NOT EQUIVALENT d .

General Case for a Body Alone or With Lifting Surfaces

For the more general case of a body alone or with lifting surfaces where the cross-sectional shape can vary along the body length, a procedure somewhat similar to that of reference 9 is suggested. However, for the general case, ratios of $(C_n/C_{n_0})_{SB}$ and $(C_n/C_{n_0})_{Newt}$ at axial stations along the body length must be used, and the crossflow terms predicted from slender-body potential theory and from viscous crossflow theory must be written in integral form. For positive dA/dx values,

$$C_N = \frac{\sin 2\alpha \cos \frac{\alpha}{2}}{A_r} \int_0^{\ell} \left(\frac{C_n}{C_{n_o}} \right)_{SB} \frac{dA}{dx} dx + \frac{2\eta C_{d_n} \sin^2 \alpha}{A_r} \int_0^{\ell} \left(\frac{C_n}{C_{n_o}} \right)_{Newt} r dx \quad (7)$$

and

$$C_m = \frac{\sin 2\alpha \cos \frac{\alpha}{2}}{A_r X} \int_0^{\ell} \left(\frac{C_n}{C_{n_o}} \right)_{SB} \frac{dA}{dx} (x_m - x) dx + \frac{2\eta C_{d_n} \sin^2 \alpha}{A_r X} \int_0^{\ell} \left(\frac{C_n}{C_{n_o}} \right)_{Newt} r (x_m - x) dx \quad (8)$$

In equations (7) and (8) the first terms (from slender-body theory) are not applicable, as written, for winged-body sections where the body dA/dx values are zero or negative. For such uses, procedures similar to those suggested in reference 16 probably should be employed to account for the potential-flow contribution of the wing to C_N and C_m . Also, for many wing-body-tail configurations, effects of vortices from body and forward lifting surfaces should be considered, and a vortex interference procedure similar to that of reference 16 probably should be formulated in conjunction with the present method.

For some applications it might be preferable to write C_N in a form similar to equation (1). When this is done,

$$C_N = \left(\frac{A_b}{A_r} \sin 2\alpha \cos \frac{\alpha}{2} \right) \left[\frac{1}{\ell} \int_0^{\ell} \left(\frac{C_n}{C_{n_o}} \right)_{SB} dx \right] + \left(\eta C_{d_n} \frac{A_p}{A_r} \sin^2 \alpha \right) \left[\frac{1}{\ell} \int_0^{\ell} \left(\frac{C_n}{C_{n_o}} \right)_{Newt} dx \right] \quad (9)$$

where the terms $(1/\ell) \int_0^{\ell} (C_n/C_{n_o})_{SB} dx$ and $(1/\ell) \int_0^{\ell} (C_n/C_{n_o})_{Newt} dx$, represent average values of $(C_n/C_{n_o})_{SB}$ and $(C_n/C_{n_o})_{Newt}$ over the body length.

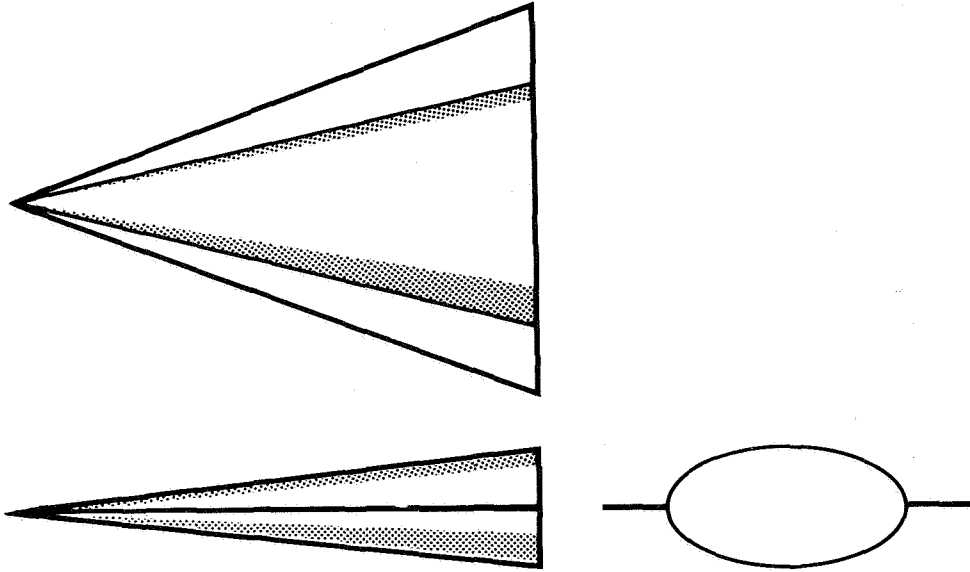
Special Case for an Elliptic Cone With Triangular Wing

For a cone of elliptic cross section with a triangular (delta) wing of the same length as the cone (sketch (b)), equations (7) and (8) for C_N and C_m simplify to equations (1) and (3), but values of $(C_N/C_{N_o}) = (C_m/C_{m_o})$ for the wing-body cross section must be used. In addition, further refinement to the slender-body term appears warranted.

Reference 17 shows that slender-body theory for triangular-winged bodies can be modified to give results comparable to linearized theory. This is accomplished merely by multiplying the slender-body result by a modification factor λ . This factor is the ratio of the lift of the wing alone by linearized theory to that by slender-body theory and is given by

$$\left. \begin{aligned} \lambda &= \frac{1}{E(\sqrt{1 - \beta^2 \tan^2 \epsilon})} \quad \text{for } \beta \tan \epsilon \leq 1 \quad (\text{subsonic leading edge}) \\ \text{and} \\ \lambda &= \frac{2}{\pi \beta \tan \epsilon} \quad \text{for } \beta \tan \epsilon \geq 1 \quad (\text{supersonic leading edge}) \end{aligned} \right\} \quad (10)$$

Here $E(\)$ is a complete elliptic integral of the second kind.



Sketch (b)

Equations (1) and (3) thus can be modified to give

$$C_N = \left(\frac{A_b}{A_r} \sin 2\alpha \cos \frac{\alpha}{2} \right) \left(\frac{C_N}{C_{N_o}} \right)_{SB} \lambda + \left(\eta C_{dn} \frac{A_p}{A_r} \sin^2 \alpha \right) \left(\frac{C_N}{C_{N_o}} \right)_{Newt} \quad (11)$$

and

$$C_m = \left[\frac{V - A_b(\ell - x_m)}{A_r X} \right] \left(\sin 2\alpha \cos \frac{\alpha}{2} \right) \left(\frac{C_m}{C_{m_o}} \right)_{SB} \lambda + \left[\eta C_{dn} \frac{A_p}{A_r} \left(\frac{x_m - x_c}{X} \right) \sin^2 \alpha \right] \left(\frac{C_m}{C_{m_o}} \right)_{Newt} \quad (12)$$

where

$$\left(\frac{C_N}{C_{N_o}} \right)_{SB} = \left(\frac{C_m}{C_{m_o}} \right)_{SB} = \left(\frac{C_n}{C_{n_o}} \right)_{SB}$$

and

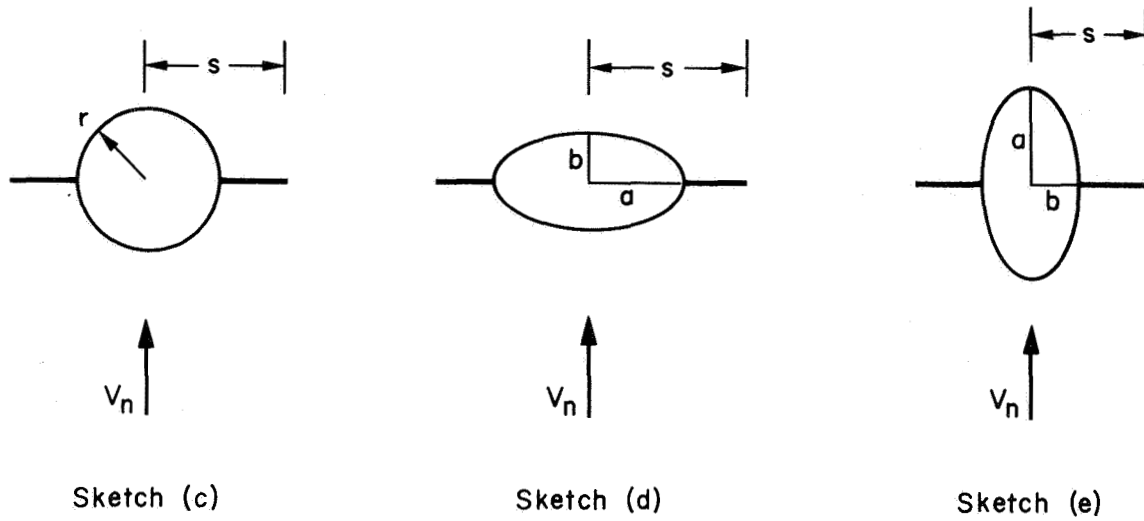
$$\left(\frac{C_N}{C_{N_o}} \right)_{Newt} = \left(\frac{C_m}{C_{m_o}} \right)_{Newt} = \left(\frac{C_n}{C_{n_o}} \right)_{Newt}$$

Formulas for computing values of $(C_n/C_{n_o})_{SB}$ and $(C_n/C_{n_o})_{Newt}$ for winged-elliptic cross sections are presented next. They are not restricted in their use, however, only to winged-elliptic cones.

Formulas and Values of $(C_n/C_{n_o})_{SB}$ and $(C_n/C_{n_o})_{Newt}$ for Winged-Elliptic Cross Sections

$(C_n/C_{n_o})_{SB}$ formulas.— From slender-body theory (e.g., refs. 18-21) the ratio of C_n for a winged-body cross section to that for the equivalent (same area) circular-body cross section can be

determined for many cross-sectional shapes. In the present study $(C_n/C_{n_0})_{SB}$ expressions have been determined for winged-circular and winged-elliptic cross sections (see sketches (c), (d), and (e)).



For a winged-circular cross section with the wing planform perpendicular to the crossflow velocity V_n (sketch (c)),

$$\left(\frac{C_n}{C_{n_0}}\right)_{SB} = \frac{s^2}{r^2} + \frac{r^2}{s^2} - 1 \quad (13)$$

For a winged-elliptic cross section with the semimajor axis a and wing planform perpendicular to the crossflow velocity V_n (sketch (d)),

$$\left(\frac{C_n}{C_{n_0}}\right)_{SB} = \frac{1}{ab} (k_1^2 + a^2) \quad (14)$$

where

$$k_1 = \sigma_1 - \frac{(a+b)^2}{4\sigma_1}$$

and

$$\sigma_1 = \frac{1}{2}(s + \sqrt{s^2 + b^2 - a^2})$$

For a winged-elliptic cross section with the semiminor axis b and wing planform perpendicular to the crossflow velocity V_n (sketch (e)),

$$\left(\frac{C_n}{C_{n_0}}\right)_{SB} = \frac{1}{ab} (k_2^2 + b^2) \quad (15)$$

where

$$k_2 = \sigma_2 - \frac{(a+b)^2}{4\sigma_2}$$

and

$$\sigma_2 = \frac{1}{2}(s + \sqrt{s^2 + a^2 - b^2})$$

$(C_n/C_{n_0})_{Newt}$ formulas.— From Newtonian impact theory, $(C_n/C_{n_0})_{Newt}$ expressions also have been derived for winged-circular and winged-elliptic cross sections.

For a winged-circular cross section with the wing planform perpendicular to the crossflow velocity V_n (sketch (c)),

$$\left(\frac{C_n}{C_{n_0}}\right)_{Newt} = \frac{3}{2} \left(\frac{s}{r} - \frac{1}{3}\right) \quad (16)$$

For a winged-elliptic cross section with the semimajor axis a and wing planform perpendicular to the crossflow velocity V_n (sketch (d)),

$$\left(\frac{C_n}{C_{n_0}}\right)_{Newt} = \frac{3}{2} \sqrt{\frac{a}{b}} \left\{ \frac{-b^2/a^2}{\left(1 - \frac{b^2}{a^2}\right)^{3/2}} \log \left[\frac{a}{b} \left(1 + \sqrt{1 - \frac{b^2}{a^2}}\right) \right] + \frac{1}{1 - \frac{b^2}{a^2}} + \frac{s}{a} - 1 \right\} \quad (17)$$

For a winged-elliptic cross section with the semiminor axis b and wing planform perpendicular to the crossflow velocity V_n (sketch (e)),

$$\left(\frac{C_n}{C_{n_0}}\right)_{Newt} = \frac{3}{2} \sqrt{\frac{b}{a}} \left[\frac{a^2/b^2}{\left(\frac{a^2}{b^2} - 1\right)^{3/2}} \tan^{-1} \left(\sqrt{\frac{a^2}{b^2} - 1} \right) - \frac{1}{\frac{a^2}{b^2} - 1} + \frac{s}{b} - 1 \right] \quad (18)$$

Values of $(C_n/C_{n_0})_{SB}$ and $(C_n/C_{n_0})_{Newt}$ — From equations (13) through (18), values of $(C_n/C_{n_0})_{SB}$ and $(C_n/C_{n_0})_{Newt}$ have been computed for elliptic cross sections alone and with wings. The results are plotted and compared in figures 1 through 4.

In figure 1 the variation of (C_n/C_{n_0}) with axis ratio a/b is given for an elliptic cross section without wings. As previously noted in reference 9, values of (C_n/C_{n_0}) from slender-body theory are reasonably close to those from Newtonian theory for many a/b 's of interest.

In figure 2 the variation of (C_n/C_{n_0}) with the ratio of wing semispan s to body radius r is given for a winged-circular cross section. For s/r 's less than about 2, the values from both theories are reasonably close to each other, but with further increase in s/r the values of $(C_n/C_{n_0})_{SB}$ greatly exceed those of $(C_n/C_{n_0})_{Newt}$.

In figure 3 values of (C_n/C_{n_0}) are presented for a winged-elliptic cross section with the semi-major axis a perpendicular to the crossflow velocity V_n . For the axis ratios of $a/b = 2$ and 3 , the figure gives the variation of (C_n/C_{n_0}) with the ratio of semispan s to semimajor axis a . As either a/b or s/a increases, the disagreement between the results from the theories increases.

In figure 4 values of (C_n/C_{n_0}) are presented for a winged-elliptic cross section with the semi-minor axis b perpendicular to the crossflow velocity V_n . For axis ratios of $a/b = 2$ and 3 , the variation of (C_n/C_{n_0}) with s/b is given. There is closer agreement between the values computed from the two theories for this cross section arrangement than for the arrangement where the semimajor axis and wing are perpendicular to V_n .

COMPARISON OF COMPUTED WITH EXPERIMENTAL AERODYNAMIC CHARACTERISTICS

In the present study, computed longitudinal aerodynamic force and moment characteristics have been compared with experimental results (ref. 6) for bodies with circular and elliptic cross sections and with experimental results (ref. 22) for winged-circular and winged-elliptic cones.

Models Studied and Test Conditions

Bodies with circular and elliptic cross sections.— Drawings of the studied bodies with circular and elliptic cross sections are shown in figure 5. The bodies' overall fineness ratios (l/d 's) are 6 and 10, and they all have fineness-ratio-3 noses followed by cylindrical sections. The bodies of elliptic cross section ($a/b = 2$) have the same cross-sectional area distribution as the equivalent circular bodies, and they were tested both oriented at $\varphi = 0^\circ$ and $\varphi = 90^\circ$, as shown in figure 5.

Lift, drag, and pitching-moment coefficients were measured for these bodies in the NASA Ames 1- by 3-Foot Supersonic Wind Tunnel No. 1. All bodies were tested at a free-stream Mach number M_∞ of 1.98. Only the fineness-ratio-10 bodies were tested at $M_\infty = 3.88$. The Reynolds number, based on body length, was 6.7×10^6 for the fineness-ratio-10 bodies and 4.0×10^6 for the fineness-ratio-6 bodies. The angle-of-attack range was from 0° to about 22° for the bodies at $M_\infty = 1.98$ and from 0° to about 15° for the bodies at $M_\infty = 3.88$. All drag coefficients presented in reference 6 have had the effects of base pressure removed and do not include base pressure drag.

Winged-circular and winged-elliptic cones.— Drawings of the winged-circular and winged-elliptic cones tested in reference 22 are shown in figure 6. Triangular wings of aspect ratio 1.0 and 1.5 were tested in combination with circular cones and elliptic cones, all of fineness-ratio-3.67. As shown in figure 6, the elliptic cones of $a/b = 3$ were arranged both with the semimajor axis a in the wing plane and perpendicular to it.

Lift, drag, and pitching-moment coefficients were measured for these models at M_∞ 's of 1.97 and 2.94 in the NASA Ames 1- by 3-Foot Supersonic Wind Tunnel No. 2 (a tunnel since disassembled). The Reynolds number, based on model length, was about 8.0×10^6 , and the angles of attack ranged from 0° to about 16° . All drag coefficients presented in reference 22 have had the effects of body base pressure removed and do not include base pressure drag.

Computation of Aerodynamic Characteristics

Because C_L , C_D , L/D , and x_{ac}/ℓ data are given in references 6 and 22, these terms were computed for the models and test conditions considered. Since C_N and C_A values are computed from the formulas of this report, it was necessary to compute C_L and C_D values with the transformation expressions:

$$C_L = C_N \cos \alpha - C_A \sin \alpha \quad (19)$$

$$C_D = C_N \sin \alpha + C_A \cos \alpha \quad (20)$$

In the computation of C_A from equation (2), values of $C_{A_{\alpha=0^\circ}}$ were assumed to be the same as those computed in references 6 and 22. The reader who is interested in computing values of $C_{A_{\alpha=0^\circ}}$ for ogival and conical nosed bodies of revolution and for elliptic cones is also referred to the procedures and formulas cited in reference 9.

Equations (1) and (3) were used to compute C_N and C_m values for the bodies with circular and elliptic cross sections. Equations (11) and (12) were used to compute these values for the winged-circular and winged-elliptic cones.

Comparison of Computed With Experimental Characteristics for Bodies With Circular and Elliptic Cross Sections

In figures 7 through 9, computed values of C_L , C_D , L/D , and x_{ac}/ℓ as a function of angle of attack α are compared with the experimental results for the bodies of $\ell/d = 6$ and 10 at $M_\infty = 1.98$ and $\ell/d = 10$ at $M_\infty = 3.88$. Generally, there is very good agreement of the computed with the experimental results. It is encouraging that effects of cross section (a/b), fineness ratio (ℓ/d), and Mach number (M_∞) on all of the aerodynamic characteristics are predicted so well.

Because of lack of data for α 's greater than about 20° , there is uncertainty concerning the validity of the method for use throughout the α range from 0° to 90° . However, because of the close agreement of computed with experimental results, shown in reference 9, for a series of cylinder, cone-cylinder, and ogive-cylinder bodies of revolution at α 's from 0° to 180° with $M_\infty = 2.86$, it is strongly believed that the method also will correctly predict the characteristics for the elliptic bodies throughout the α range. Nevertheless, over the M_∞ , Re , and α ranges of current interest, further testing of bodies with elliptic and other cross sections appears desirable to ascertain validity limits for the method.

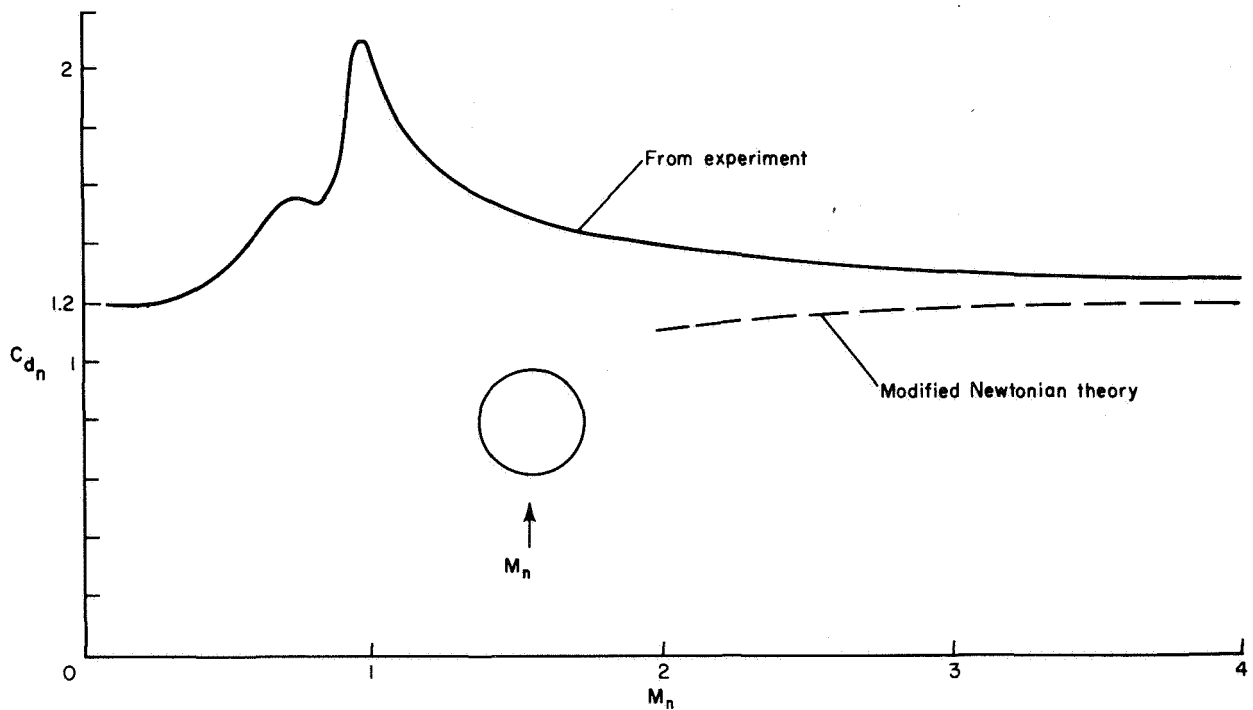
Comparison of Computed With Experimental Characteristics for Winged-Circular
and Winged-Elliptic Cones

In figures 10 through 13, computed aerodynamic characteristics are compared with the experimental results for the winged-circular and winged-elliptic cones. As for the bodies alone, the computed and experimental results generally agree. The closest agreement is at $M_\infty = 1.97$ (see figs. 10 and 11). At $M_\infty = 2.94$ (figs. 12 and 13) the method tends to overpredict C_L somewhat with increase in α . However, the agreement is still probably acceptable for most engineering studies.

In the method for computing the aerodynamic characteristics, values of crossflow drag coefficient C_{d_n} for a two-dimensional circular cylinder are used. Generally C_{d_n} is a function only of M_n ($M_n = M_\infty \sin \alpha$), except for Re greater than about 2×10^5 with M_n less than about 0.5 (see, e.g., ref. 9). With increase in M_n from 0.2 to 1, C_{d_n} increases from about 1.2 to 2, then decreases as M_∞ increases into the supersonic-hypersonic regime (see sketch (f)). At hypersonic M_n , values of C_{d_n} predicted from modified Newtonian theory agree closely with experiment. From modified Newtonian theory,

$$\begin{aligned} C_{d_n} &= \frac{2}{3} C_{p_{stag}} \\ &= 1.2 \text{ for } C_{p_{stag}} = 1.8 \end{aligned} \tag{21}$$

For M_n greater than about 4, $C_{p_{stag}} \approx 1.8$ from perfect-gas relations.



Sketch (f)

It is questionable whether the experimental variation of C_{d_n} with M_n for a circular cylinder should be used in the calculation of the aerodynamic characteristics for winged bodies. It is likely that some other variation or a constant value of C_{d_n} will give closer agreement of theory with experiment, especially at α 's where M_n is in the transonic regime.

Figure 14 indicates the effect of C_{d_n} on the prediction of C_L and L/D for the winged cones at α 's from 0° to 90° for $M_\infty = 2.94$. Computed curves are shown for the assumptions that $C_{d_n} = f(M_n)$ and $C_{d_n} = 1.2$, the value for both low subsonic and hypersonic M_n for a circular cylinder. The figure shows significant effect of C_{d_n} on the prediction of C_L for all models at α 's greater than about 15° for $M_\infty = 2.94$. There is negligible effect, however, on the prediction of L/D . Further testing of winged bodies at high angles of attack is definitely necessary to aid in the development of correct usage of the present method for computing C_L .

CONCLUDING REMARKS

An engineering-type method has been presented for estimating normal-force, axial-force, and pitching-moment coefficients for slender bodies of circular and noncircular cross section alone and with lifting surfaces. In the generalized equations that are given for C_N and C_m , ratios are required of the local normal-force coefficient per unit length for the cross section of interest to that for the equivalent (same area) circular cross section. These ratios are given both from slender-body and Newtonian theories. Formulas and numerical values of these ratios for winged-elliptic cross sections are included in this report.

Static aerodynamic characteristics computed by the method have been shown to agree closely with experimental results for slender bodies of circular and elliptic cross section and for winged-circular and winged-elliptic cones. However, because the experimental results are limited to angles of attack less than about 20° and Mach numbers only from 2 to 4, further comparison of the method with more data is needed to determine validity limits for the method.

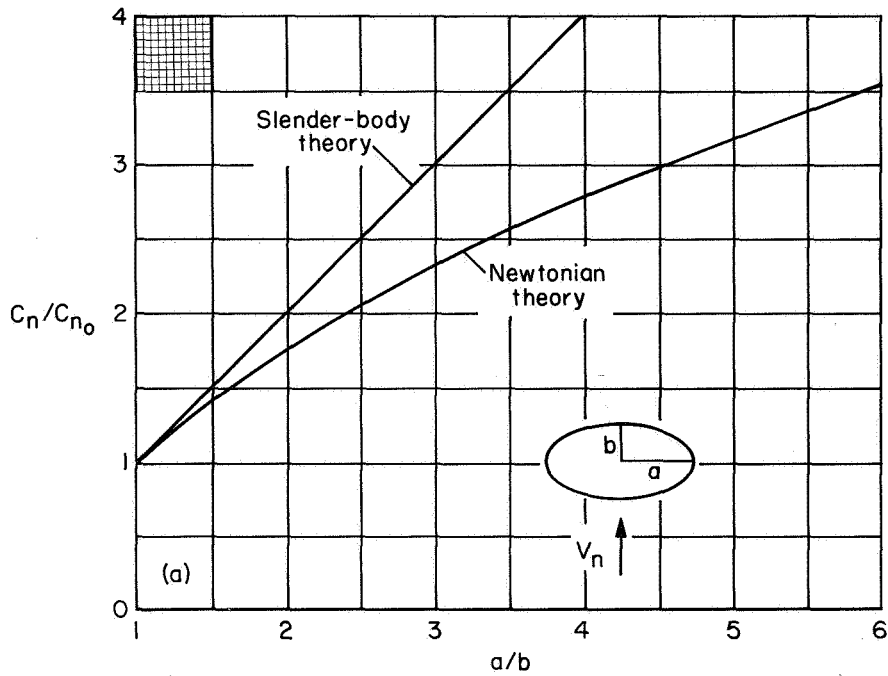
Effects of forebody-flow and wing-flow separation on downstream aerodynamic surfaces have not been included in the present study, but these effects should be investigated by representing regions of separated flow with both concentrated and distributed vortices. Then the effects of integrated forces and moments caused by varying configuration geometry can be studied numerically. However, confidence in the analytical approaches will have to be established by comparison of computed with experimental results for wing-body-tail combinations at high angles of attack (up to 90°) and at Mach and Reynolds numbers of interest.

Ames Research Center
National Aeronautics and Space Administration
Moffett Field, Calif., Dec. 13, 1972

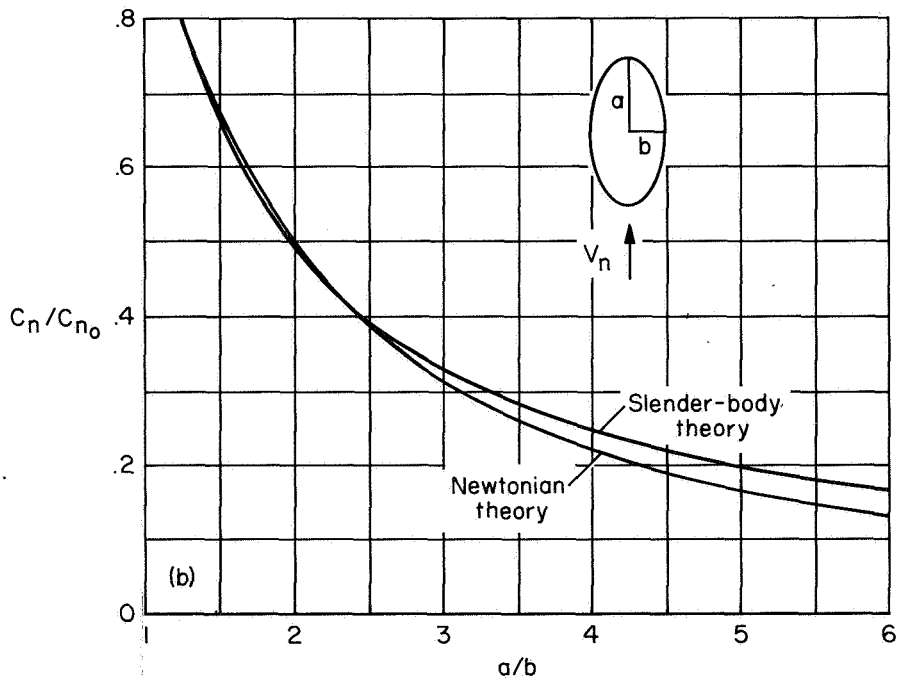
REFERENCES

1. Allen, H. Julian: Estimation of the Forces and Moments Acting on Inclined Bodies of Revolution of High Fineness Ratio. NACA RM A9126, 1949.
2. Allen, H. Julian; and Perkins, Edward W.: A Study of Effects of Viscosity on Flow Over Slender Inclined Bodies of Revolution. NACA Rep. 1048, 1951.
3. Perkins, Edward W.; and Kuehn, Donald M.: Comparison of the Experimental and Theoretical Distributions of Lift on a Slender Inclined Body of Revolution at $M = 2$. NACA TN 3715, 1956.
4. Perkins, Edward W.; and Jorgensen, Leland, H.: Comparison of Experimental and Theoretical Normal-Force Distributions (Including Reynolds Number Effects) on an Ogive-Cylinder Body at Mach Number 1.98. NACA TN 3716, 1956.
5. Jorgensen, Leland H.; and Perkins, Edward W.: Investigation of Some Wake Vortex Characteristics of an Inclined Ogive-Cylinder Body at Mach Number 2. NACA Rep. 1371, 1958.
6. Jorgensen, Leland H.: Inclined Bodies of Various Cross Sections at Supersonic Speeds. NASA MEMO 10-3-58A, 1958.
7. Jorgensen, Leland H.; and Treon, Stuart L.: Measured and Estimated Aerodynamic Characteristics for a Model of a Rocket Booster at Mach Numbers From 0.6 to 4 and at Angles of Attack From 0° to 180° . NASA TM X-580, 1961.
8. Saffel, Bernard F., Jr.; Howard, Millard L.; and Brooks, Eugene N., Jr.: Method for Predicting the Static Aerodynamic Characteristics of Typical Missile Configurations for Angles of Attack to 180 Degrees. Report 3645, Naval Ship Research and Development Center, March 1971.
9. Jorgensen, Leland H.: Prediction of Static Aerodynamic Characteristics for Space-Shuttle-Like and Other Bodies at Angles of Attack From 0° to 180° . NASA TN D-6996, 1973.
10. Goldstein, Sydney: Modern Developments in Fluid Dynamics. Oxford, The Clarendon Press, vol. 2, sec. 195, 1938, pp. 439-440.
11. Wieselsberger, C.: New Data on the Laws of Fluid Resistance. NACA TN 84, 1922.
12. Lindsey, W. F.: Drag of Cylinders of Simple Shapes. NACA Rep. 619, 1938.
13. Delany, Noel K.; and Sorensen, Norman E.: Low-Speed Drag of Cylinders of Various Shapes. NACA TN 3038, 1953.
14. Polhamus, Edward C.; Getler, Edward W.; and Grunwald, Kalman J.: Pressure and Force Characteristics of Non-circular Cylinders as Affected by Reynolds Number With a Method Included for Determining the Potential Flow About Arbitrary Shapes. NASA TR R-46, 1959.
15. Polhamus, Edward C.: Effect of Flow Incidence and Reynolds Number on Low-Speed Aerodynamic Characteristics of Several Noncircular Cylinders With Applications to Directional Stability and Spinning. NASA TR R-29, 1959.

16. Pitts, William C.; Nielsen, Jack N.; and Kaattari, George E.: Lift and Center of Pressure of Wing-Body-Tail Combinations at Subsonic, Transonic, and Supersonic Speeds. NACA Rep. 1307, 1957.
17. Nielsen, Jack N.; Katzen, Elliott D.; and Tang, Kenneth K.: Lift and Pitching-Moment Interference Between a Pointed Cylindrical Body and Triangular Wings of Various Aspect Ratios at Mach Numbers of 1.50 and 2.02: NACA TN 3795, 1956.
18. Bryson, Arthur E., Jr.: Stability Derivatives for a Slender Missile With Application to a Wing-Body-Vertical-Tail Configuration. Jour. Aero. Sci., vol. 20, no. 5, May 1953, pp. 297-308.
19. Bryson, Arthur E., Jr.: Evaluation of the Inertia Coefficients of the Cross Section of a Slender Body. Jour. Aero. Sci., vol. 21, no. 6, June 1954, pp. 424-427.
20. Bryson, Arthur E., Jr.: The Aerodynamic Forces on a Slender Low (or High) Wing, Circular Body, Vertical Tail Configuration. Jour. Aero. Sci., vol. 21, no. 8, Aug. 1954, pp. 574-575.
21. Nielsen, Jack N.: Missile Aerodynamics. New York, McGraw-Hill Company, Inc., 1960.
22. Jorgensen, Leland H.: Elliptic Cones Alone and With Wings at Supersonic Speeds. NACA TN 4045, 1957.



(a) Semimajor axis a perpendicular to crossflow velocity V_n .



(b) Semiminor axis b perpendicular to crossflow velocity V_n .

Figure 1.— Ratio of local normal-force coefficient for an elliptic cross section to that for the equivalent circular cross section.

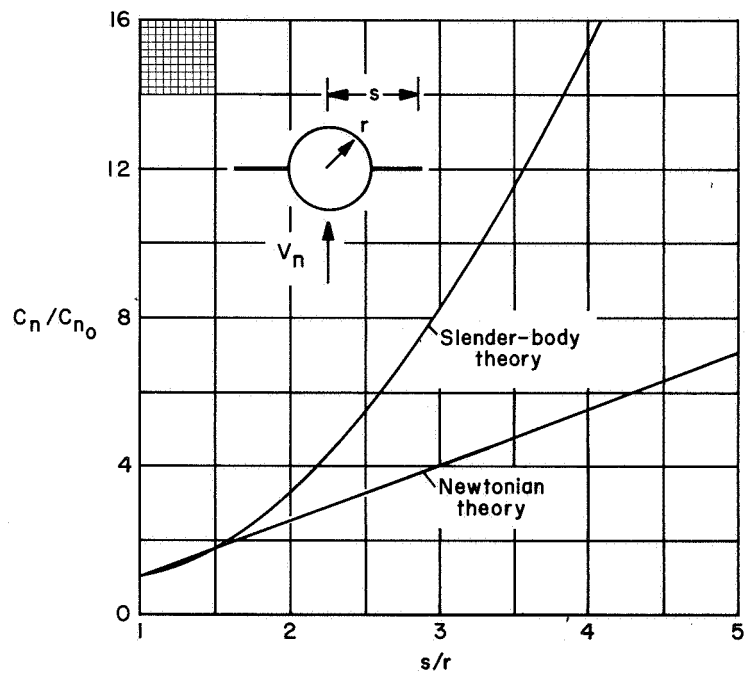
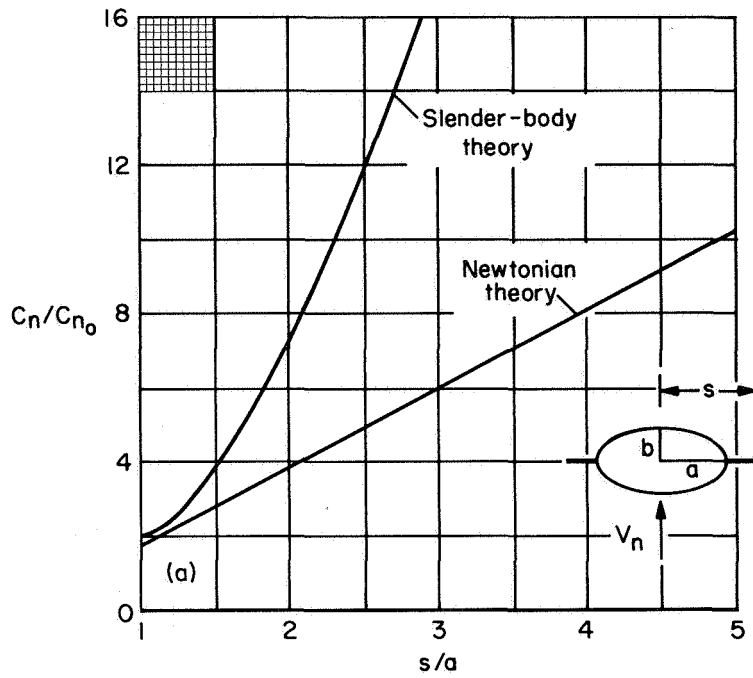
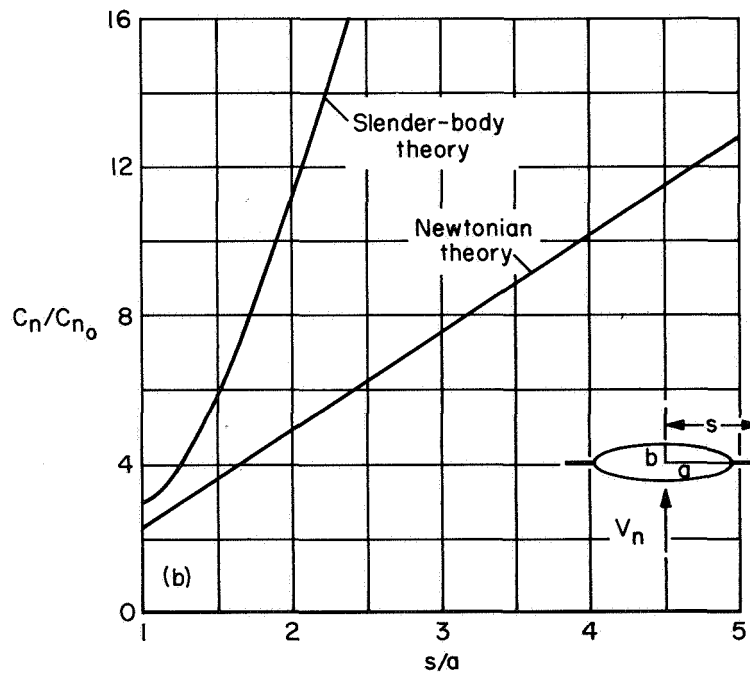


Figure 2.— Ratio of local normal-force coefficient for a winged-circular cross section to that for the equivalent circular cross section.

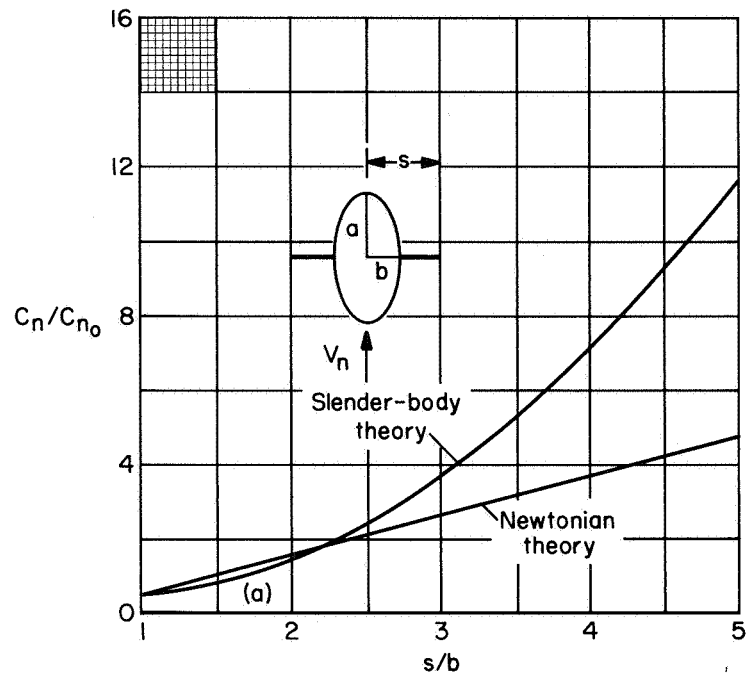


(a) $a/b = 2$

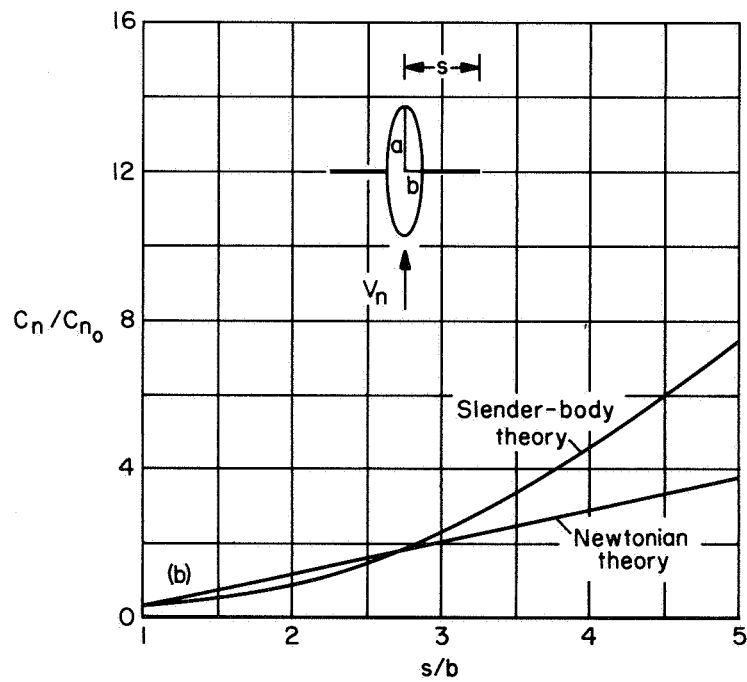


(b) $a/b = 3$

Figure 3.— Ratio of local normal-force coefficient for a winged-elliptic cross section to that for the equivalent circular cross section; semimajor axis a perpendicular to crossflow velocity V_n .



(a) $a/b = 2$



(b) $a/b = 3$

Figure 4.— Ratio of local normal-force coefficient for a winged-elliptic cross section to that for the equivalent circular cross section; semiminor axis b perpendicular to crossflow velocity V_n .

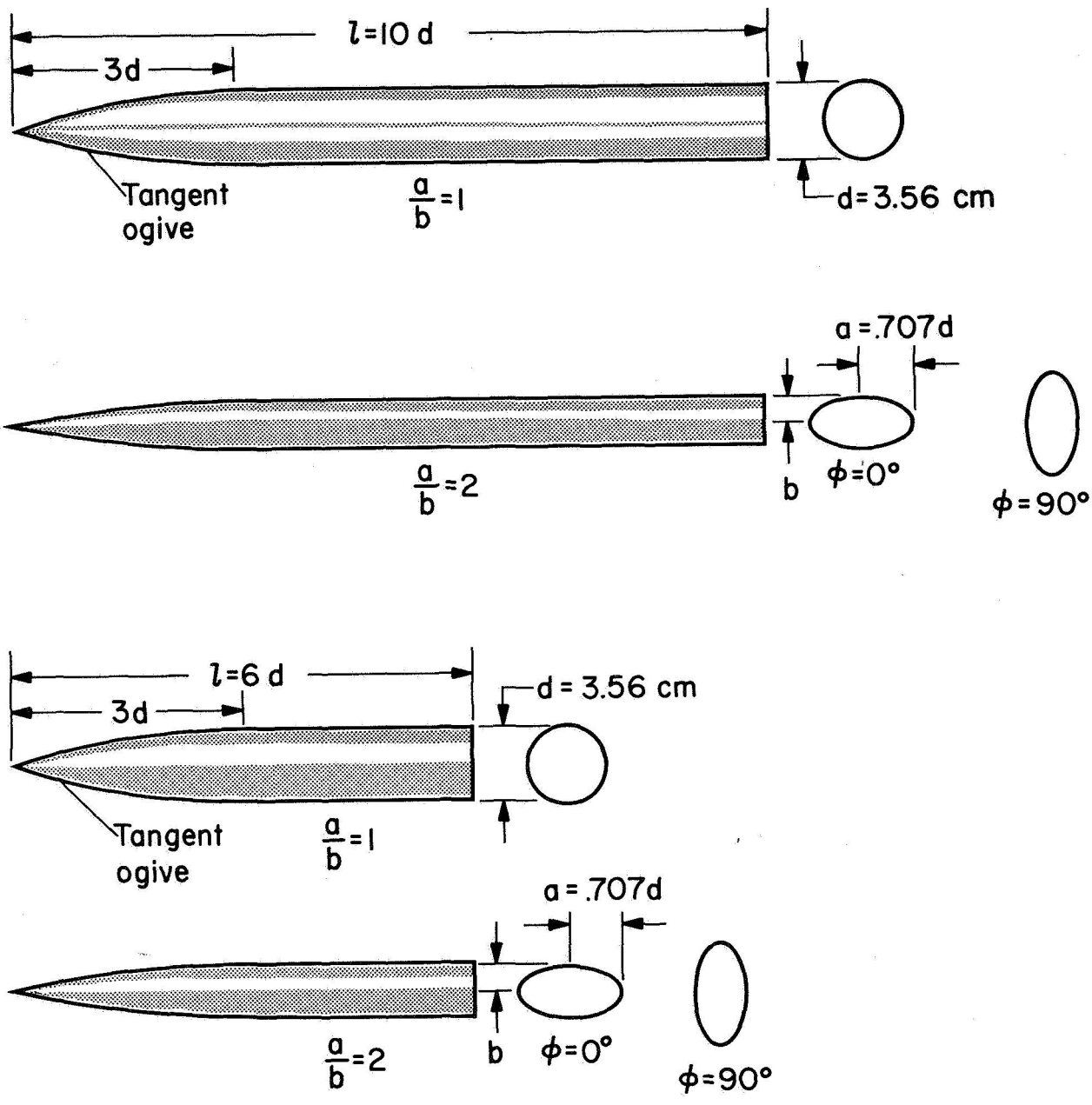
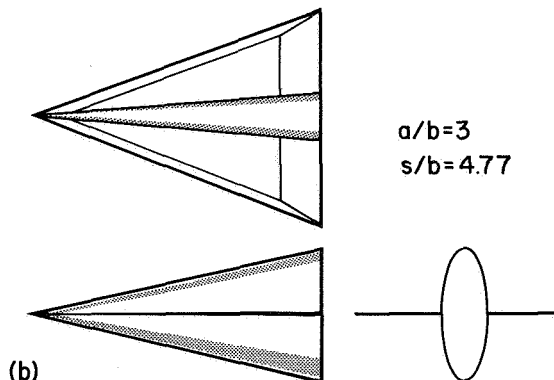
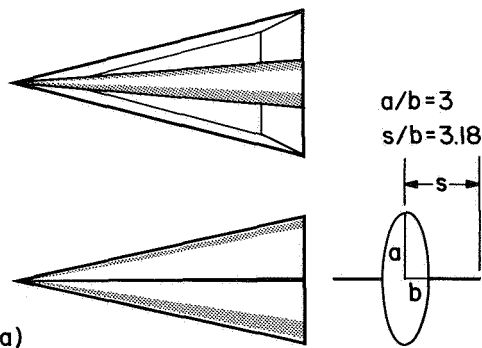
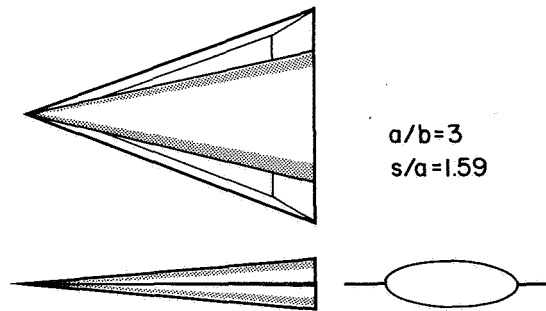
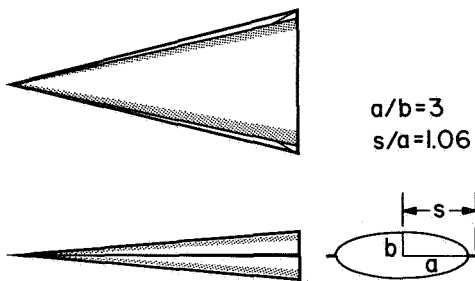
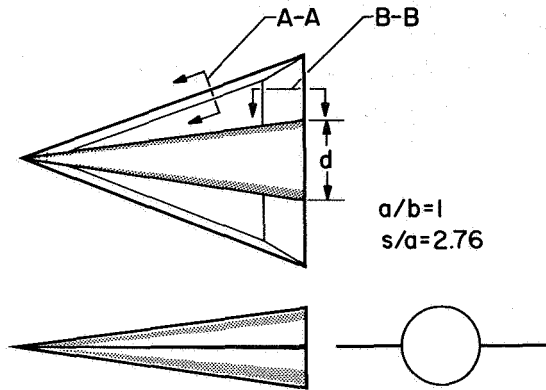
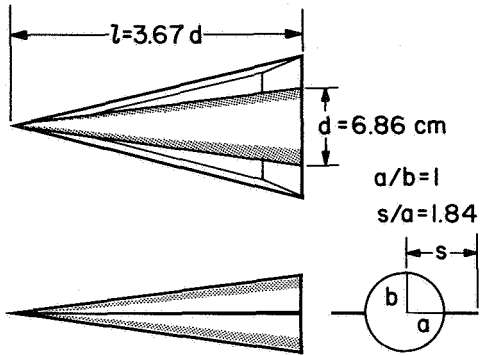
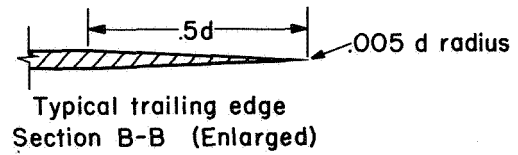
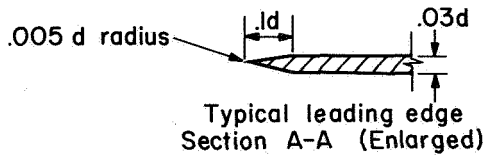


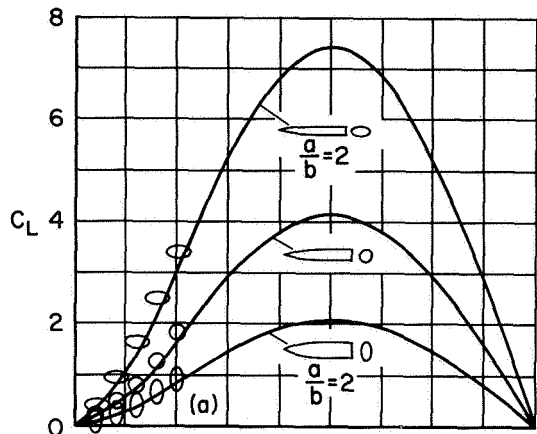
Figure 5.— Models for which the aerodynamic characteristics were measured in reference 6 and computed in the present study.



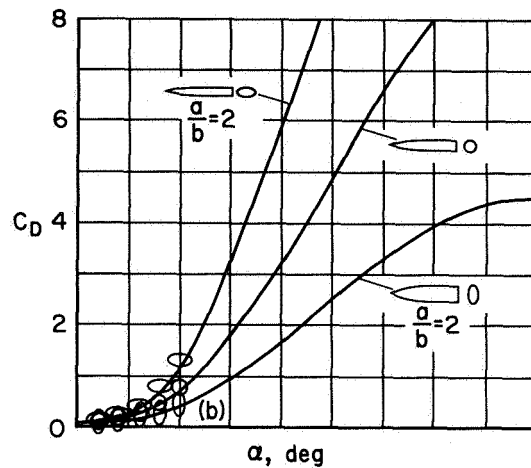
(a) Wing aspect ratio = 1.0.

(b) Wing aspect ratio = 1.5.

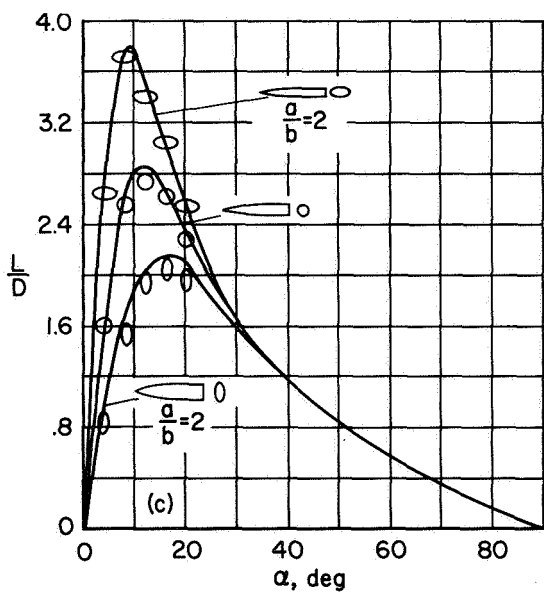
Figure 6.— Models for which the aerodynamic characteristics were measured in reference 22 and computed in the present study.



(a) Lift.

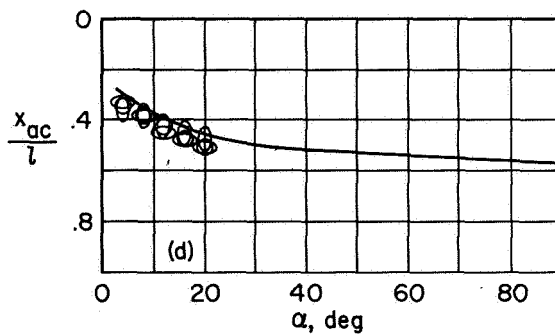


(b) Drag.



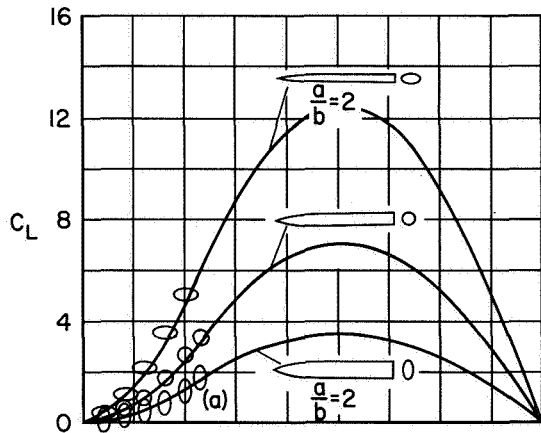
(c) Lift-drag ratio.

— Computed
 ○ ○ Experiment (ref. 6)

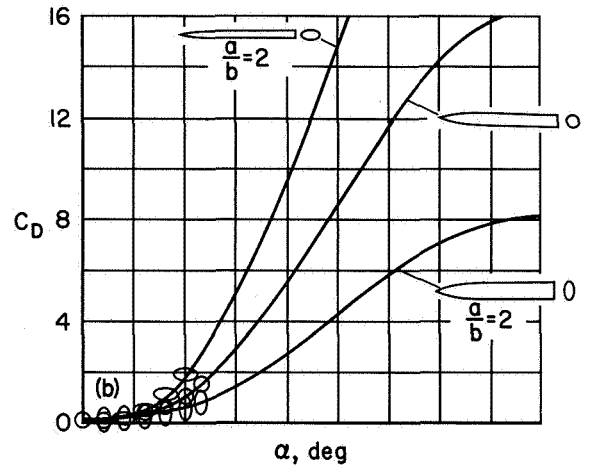


(d) Aerodynamic center.

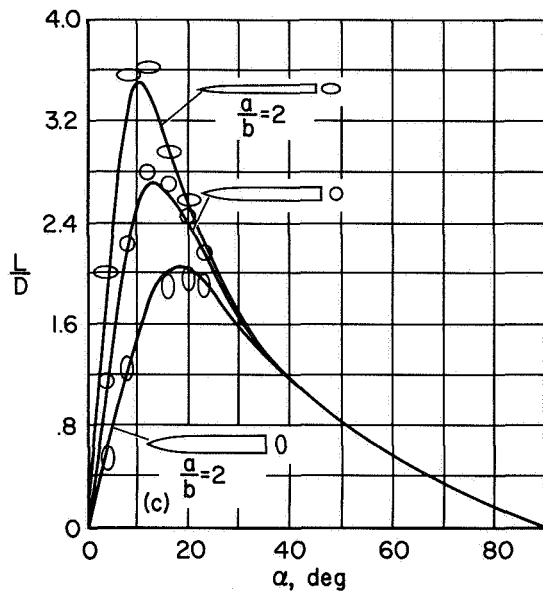
Figure 7.— Comparison of computed with experimental aerodynamic characteristics for bodies with elliptic cross sections; $L/D = 6$, $M_\infty = 1.98$, $Re = 4.0 \times 10^6$.



(a) Lift.

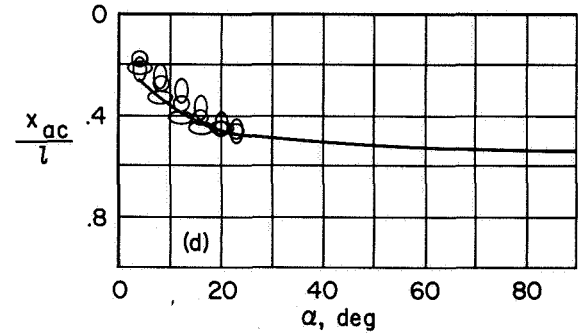


(b) Drag.



(c) Lift-drag ratio.

— Computed
 ○ ○ Experiment (ref. 6)



(d) Aerodynamic center.

Figure 8.— Comparison of computed with experimental aerodynamic characteristics for bodies with elliptic cross sections; $L/D = 10$, $M_\infty = 1.98$, $Re = 6.7 \times 10^6$.

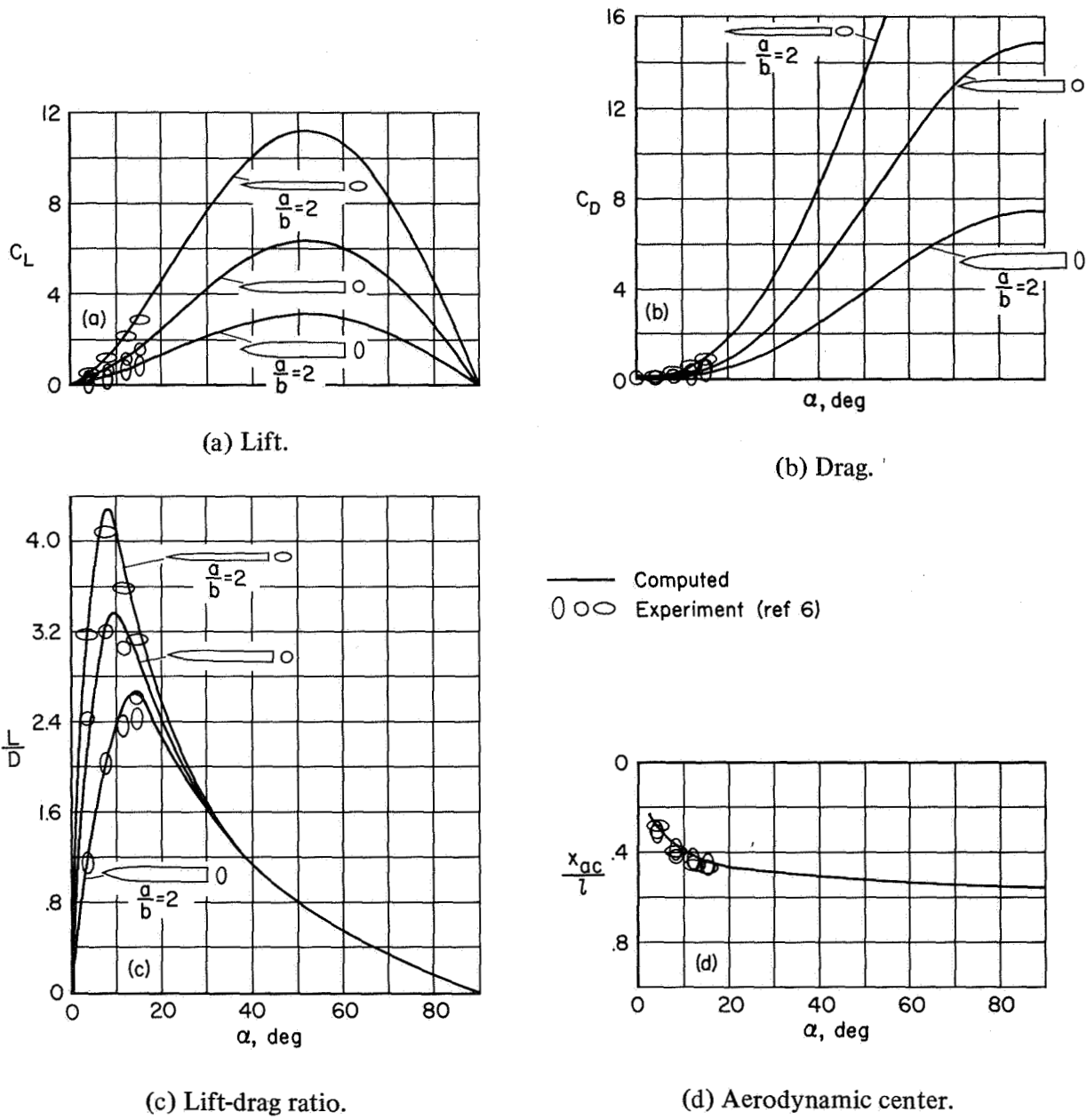
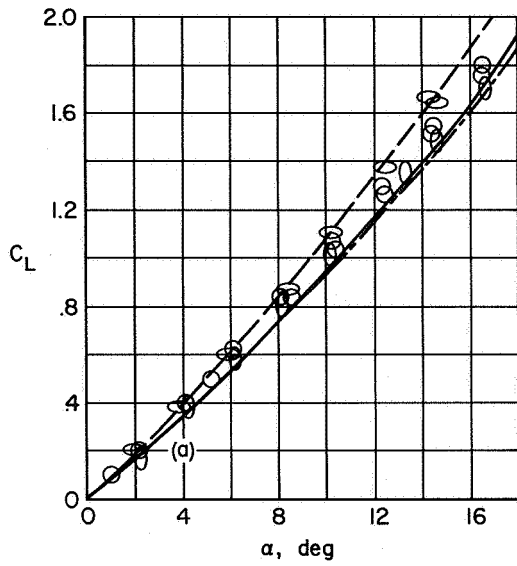
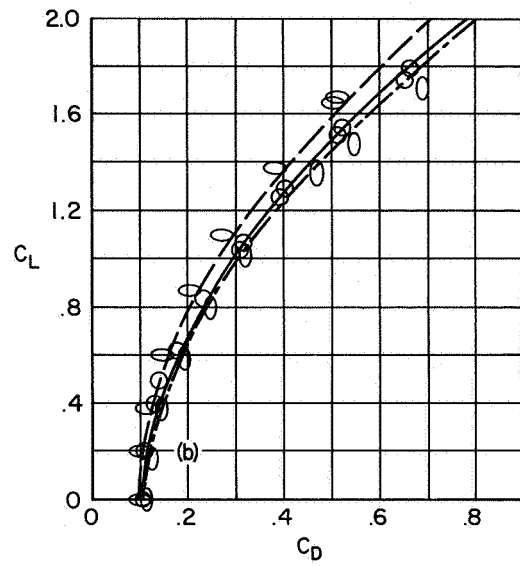


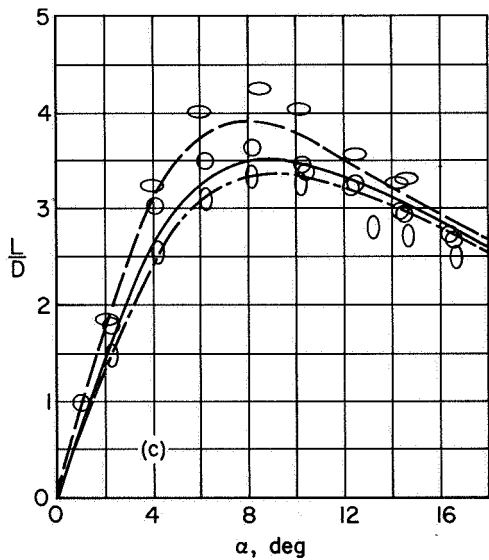
Figure 9.— Comparison of computed with experimental aerodynamic characteristics for bodies with elliptic cross sections; $L/D = 10$, $M_\infty = 3.88$, $Re = 6.7 \times 10^6$.



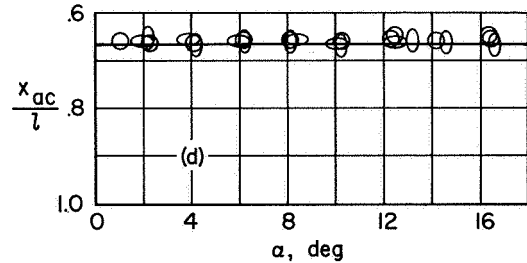
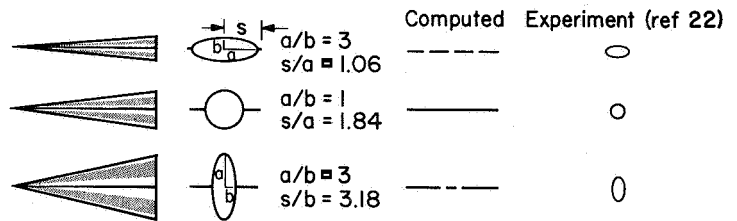
(a) Lift.



(b) Lift-drag polar.

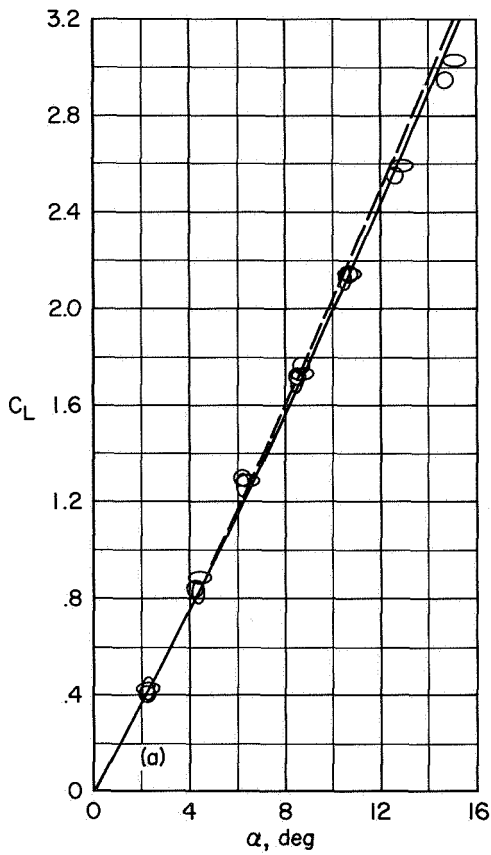


(c) Lift-drag ratio.

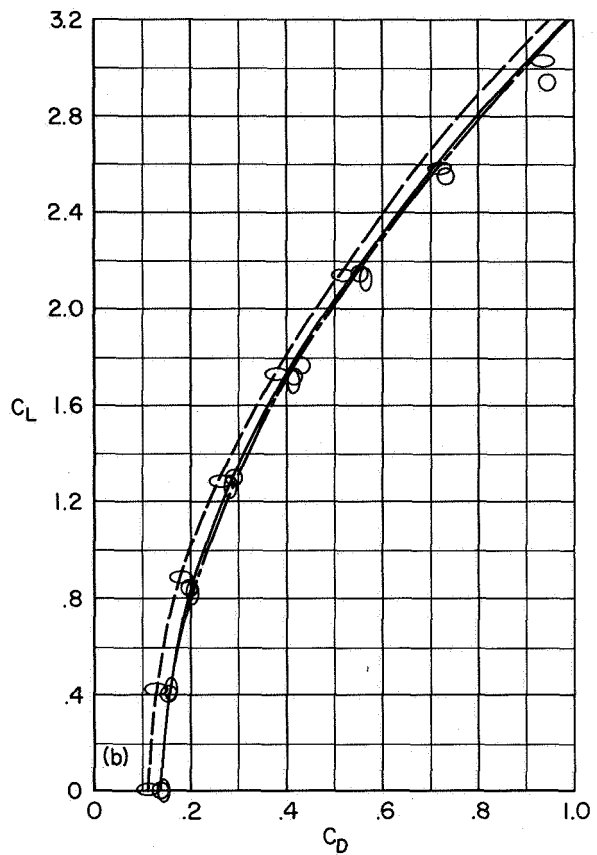


(d) Aerodynamic center.

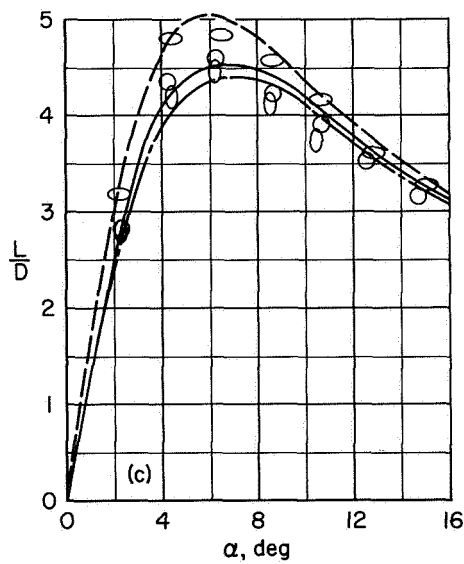
Figure 10.— Comparison of computed with experimental aerodynamic characteristics for elliptic cones with triangular wings of aspect ratio 1.0 at $M_\infty = 1.97$; $Re = 8 \times 10^6$.



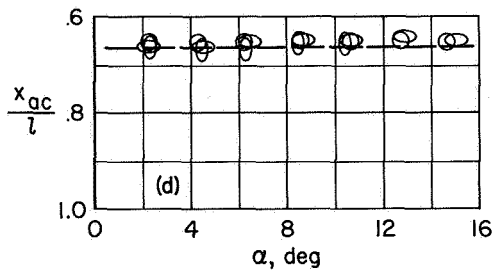
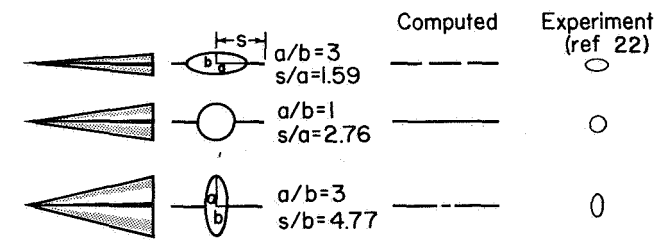
(a) Lift.



(b) Lift-drag polar.

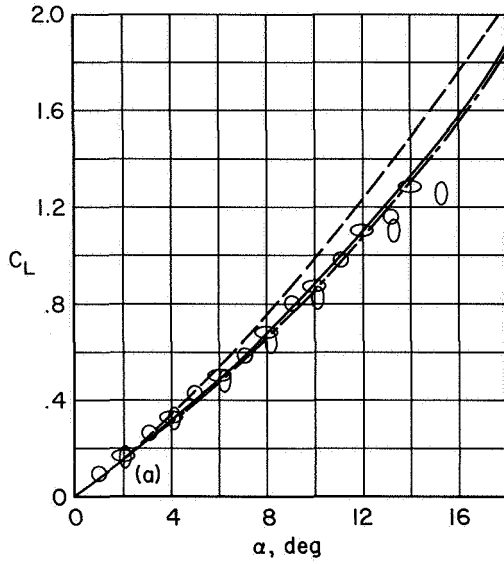


(c) Lift-drag ratio.

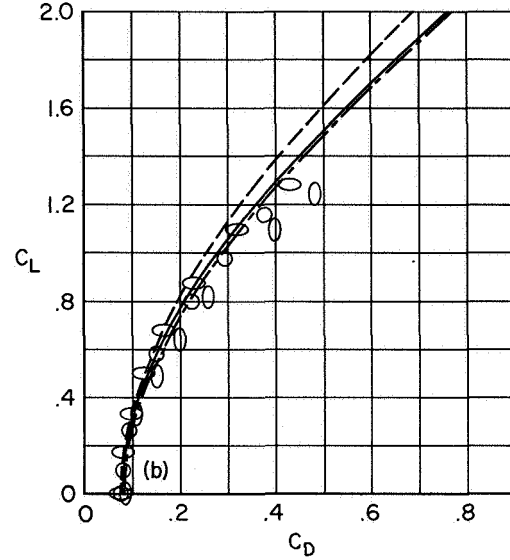


(d) Aerodynamic center.

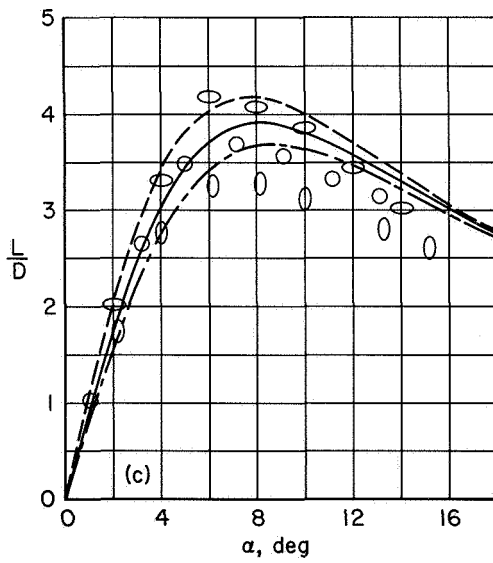
Figure 11.— Comparison of computed with experimental aerodynamic characteristics for elliptic cones with triangular wings of aspect ratio 1.5 at $M_\infty = 1.97$; $Re = 8 \times 10^6$.



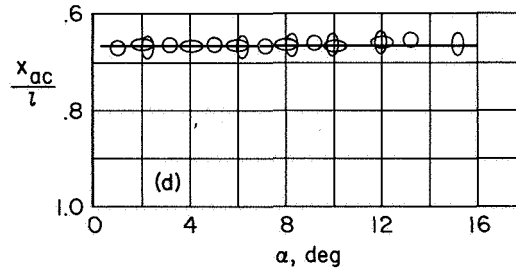
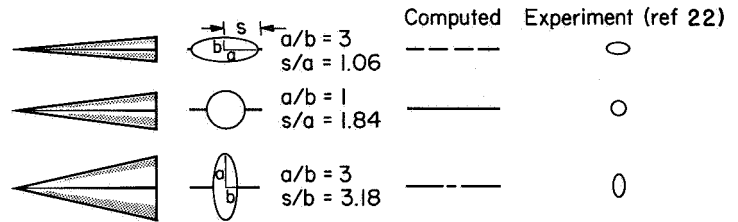
(a) Lift.



(b) Lift-drag polar.

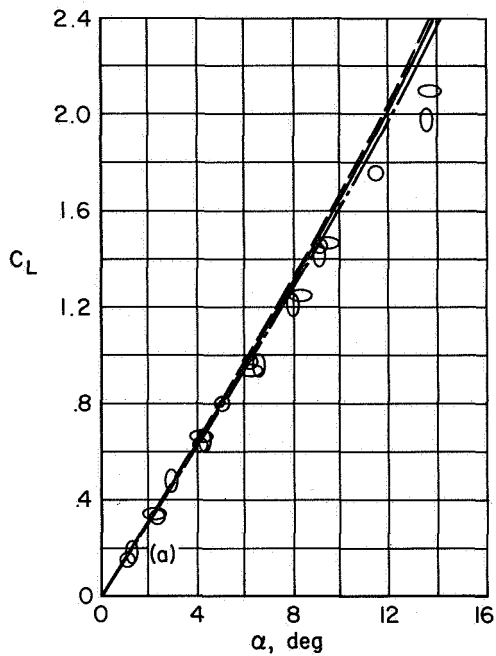


(c) Lift-drag ratio.

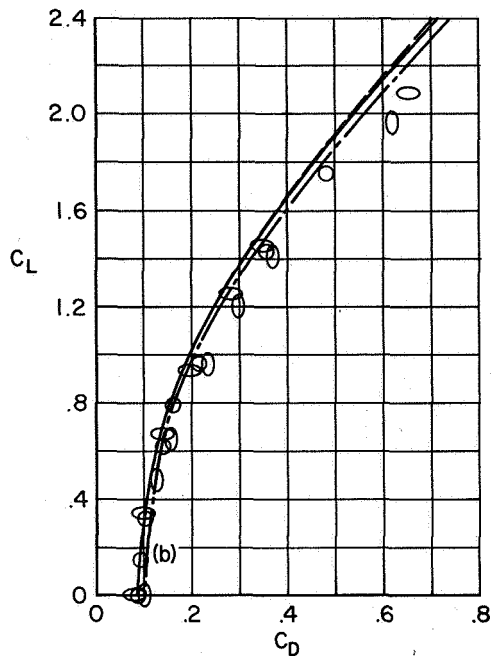


(d) Aerodynamic center.

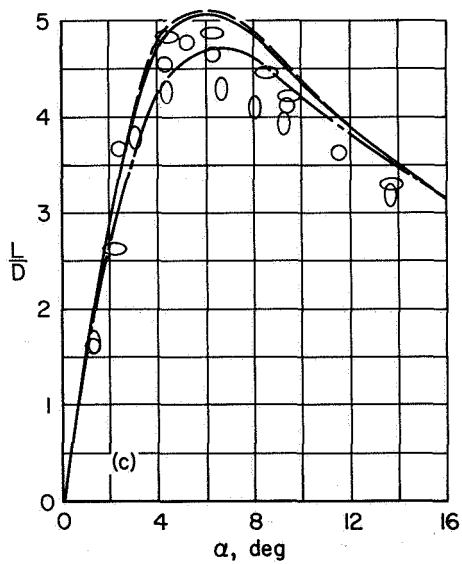
Figure 12.— Comparison of computed with experimental aerodynamic characteristics for elliptic cones with triangular wings of aspect ratio 1.0 at $M_\infty = 2.94$; $Re = 8 \times 10^6$.



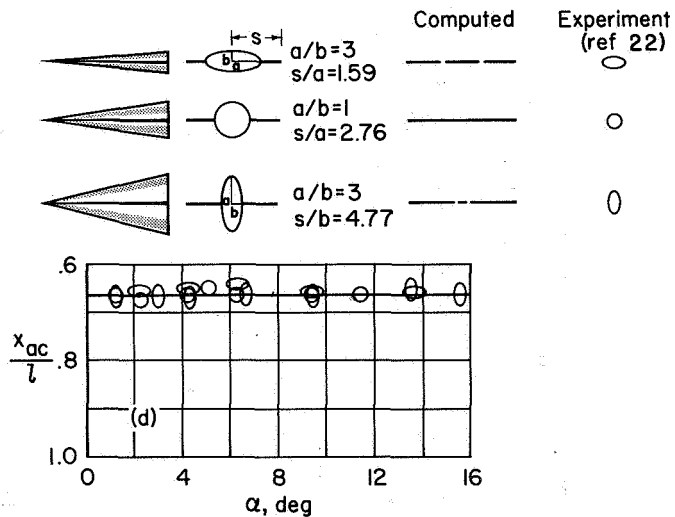
(a) Lift.



(b) Lift-drag polar.

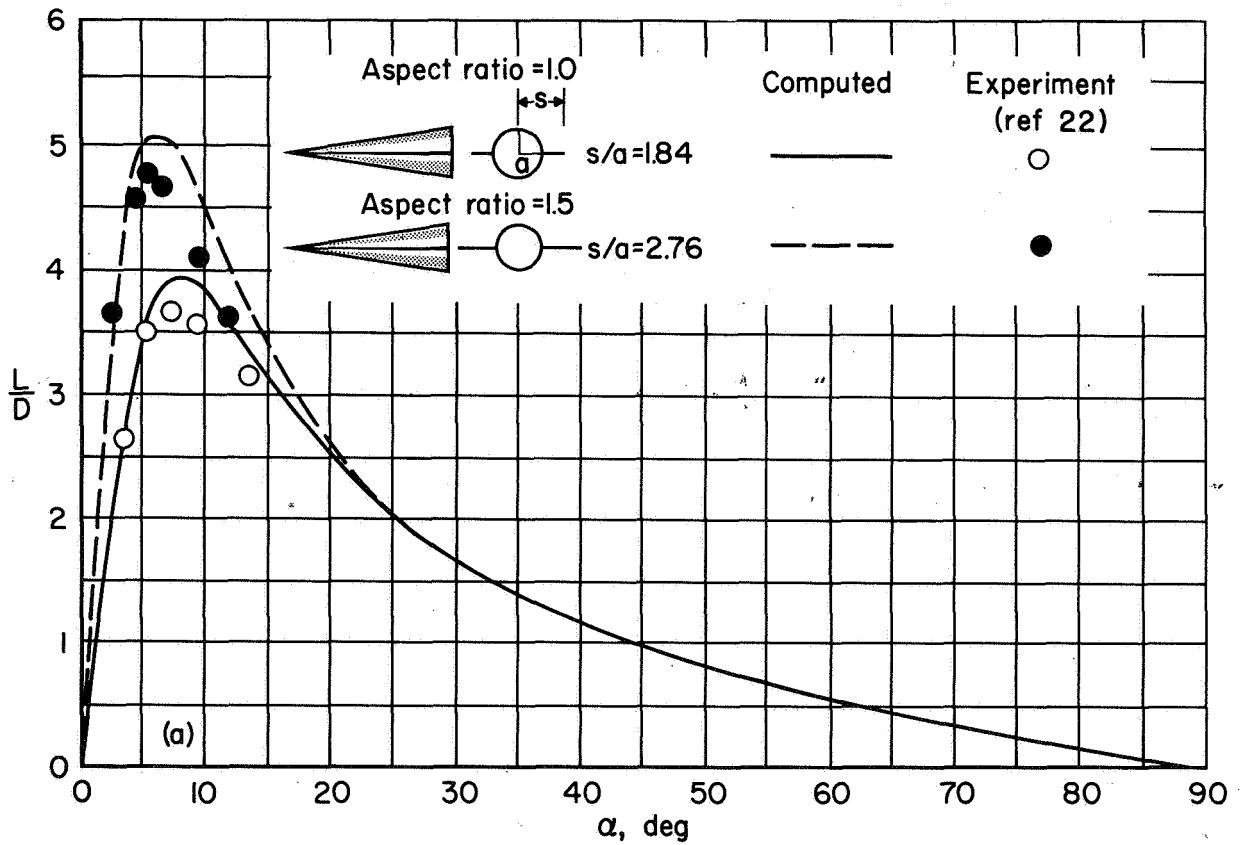
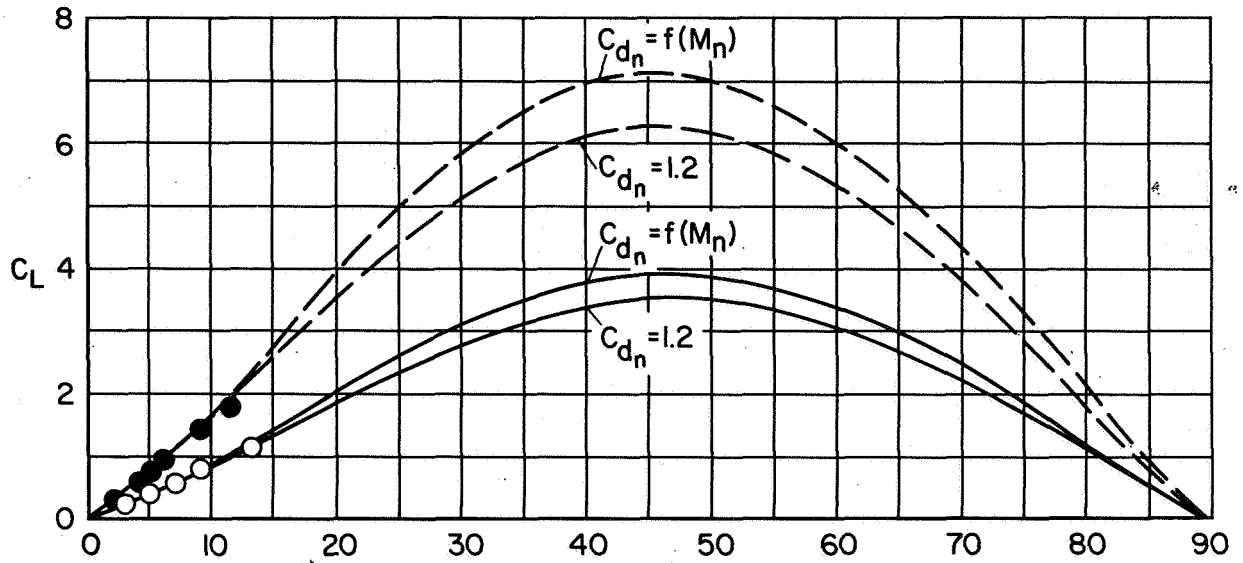


(c) Lift-drag ratio.



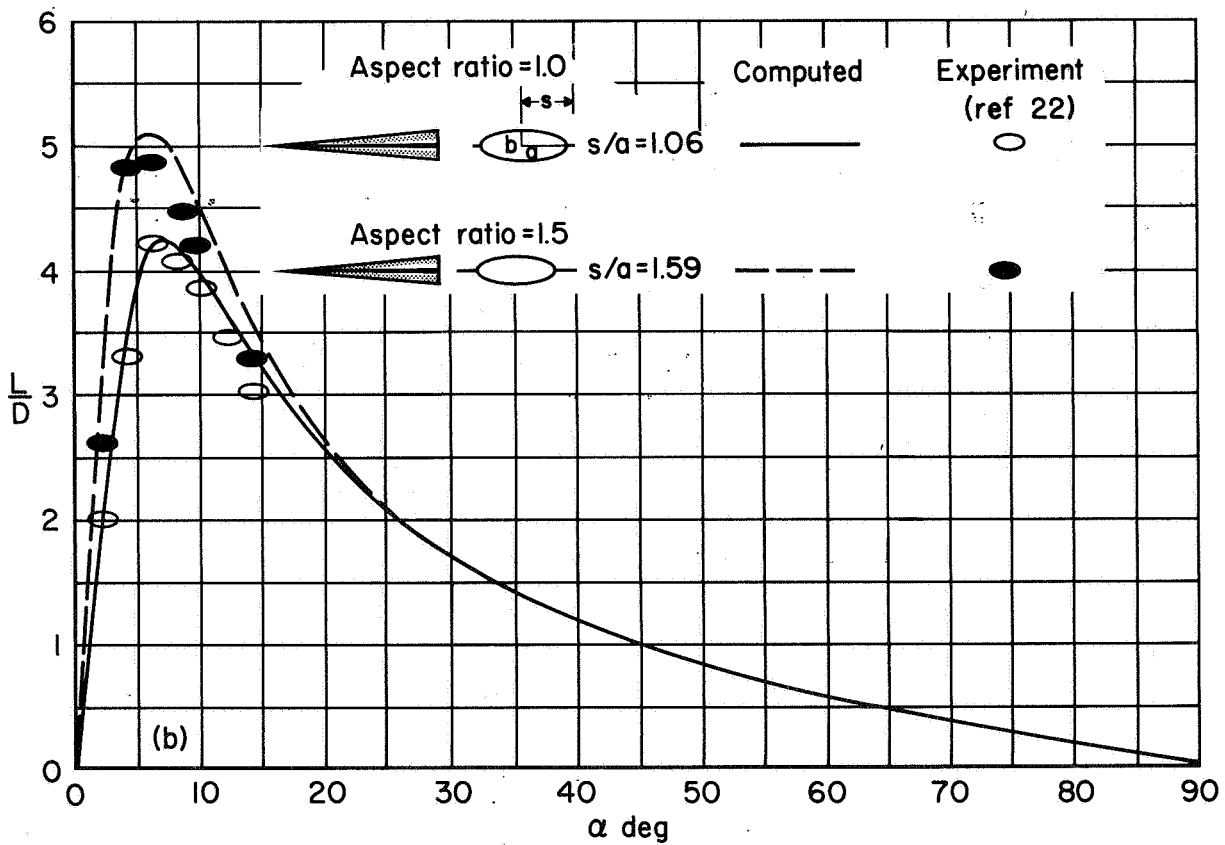
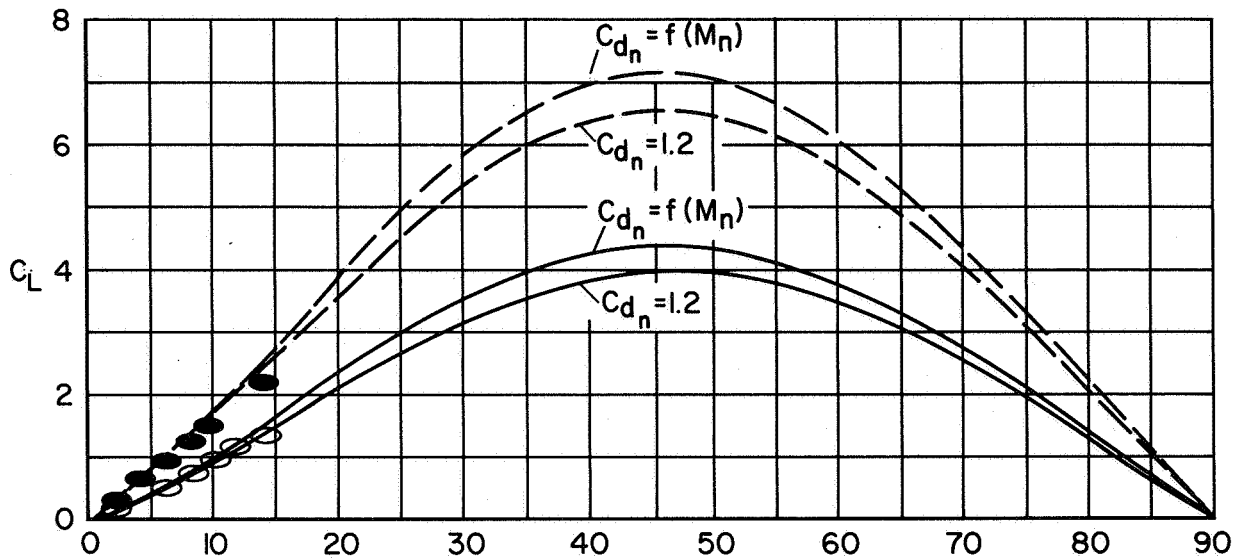
(d) Aerodynamic center.

Figure 13.— Comparison of computed with experimental aerodynamic characteristics for elliptic cones with triangular wings of aspect ratio 1.5 at $M_\infty = 2.94$; $Re = 8 \times 10^6$.



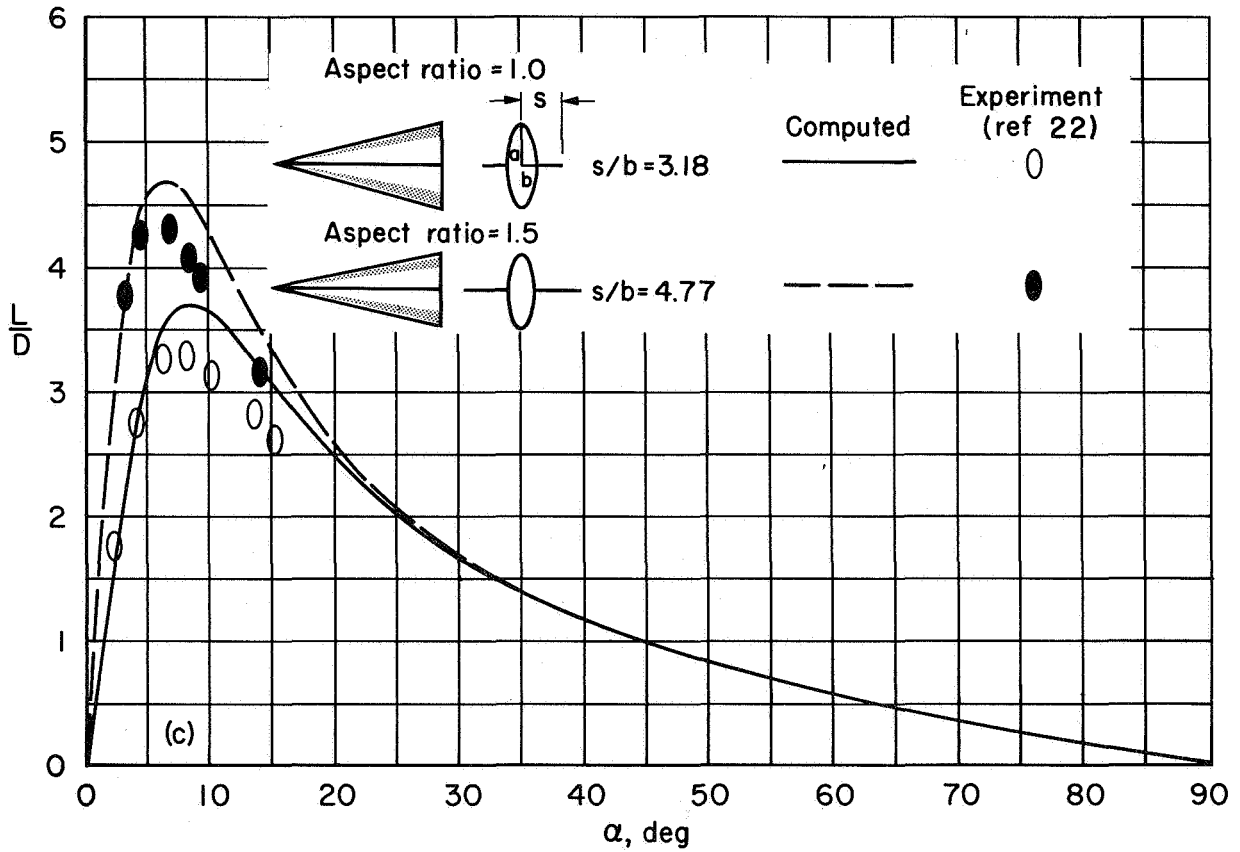
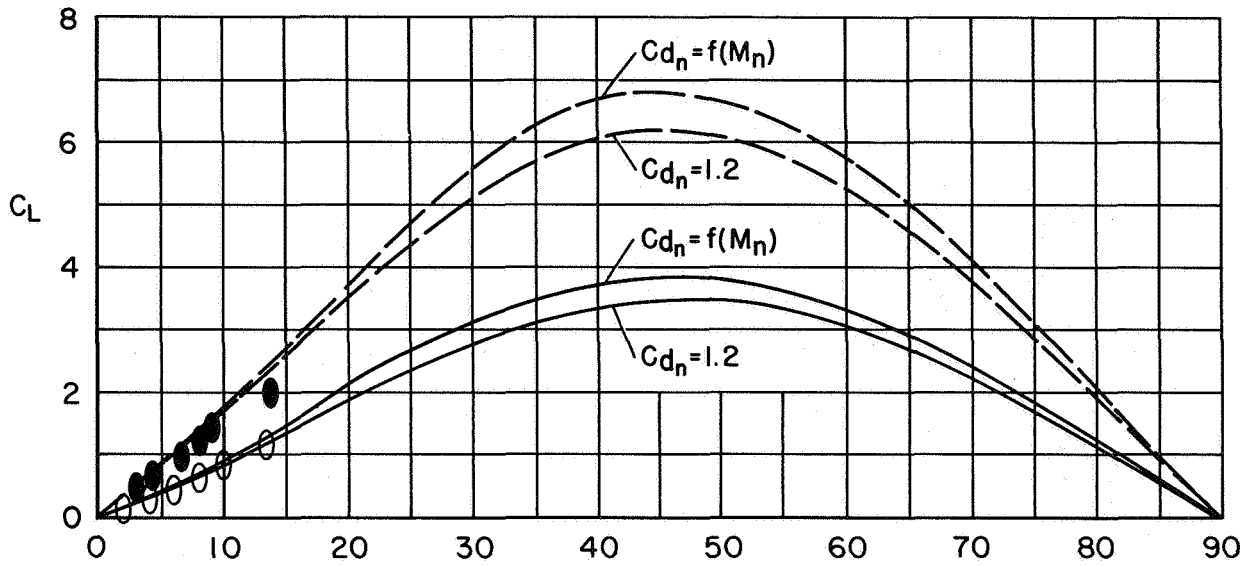
(a) Circular cone.

Figure 14.— Effect of circular-cylinder crossflow drag coefficient C_{d_n} on prediction of C_L and L/D for cones with triangular wings at α 's from 0° to 90° ; $M_\infty = 2.94$.



(b) Elliptic cone of $a/b = 3$ with a perpendicular to V_n .

Figure 14.— Continued.



(c) Elliptic cone of $a/b = 3$ with b perpendicular to V_n .

Figure 14.— Concluded.

NATIONAL AERONAUTICS AND SPACE ADMINISTRATION
WASHINGTON, D.C. 20546

OFFICIAL BUSINESS
PENALTY FOR PRIVATE USE \$300

**SPECIAL FOURTH-CLASS RATE
BOOK**

POSTAGE AND FEES PAID
NATIONAL AERONAUTICS AND
SPACE ADMINISTRATION
451



POSTMASTER: If Undeliverable (Section 158
Postal Manual) Do Not Return

"The aeronautical and space activities of the United States shall be conducted so as to contribute . . . to the expansion of human knowledge of phenomena in the atmosphere and space. The Administration shall provide for the widest practicable and appropriate dissemination of information concerning its activities and the results thereof."

—NATIONAL AERONAUTICS AND SPACE ACT OF 1958

NASA SCIENTIFIC AND TECHNICAL PUBLICATIONS

TECHNICAL REPORTS: Scientific and technical information considered important, complete, and a lasting contribution to existing knowledge.

TECHNICAL NOTES: Information less broad in scope but nevertheless of importance as a contribution to existing knowledge.

TECHNICAL MEMORANDUMS: Information receiving limited distribution because of preliminary data, security classification, or other reasons. Also includes conference proceedings with either limited or unlimited distribution.

CONTRACTOR REPORTS: Scientific and technical information generated under a NASA contract or grant and considered an important contribution to existing knowledge.

TECHNICAL TRANSLATIONS: Information published in a foreign language considered to merit NASA distribution in English.

SPECIAL PUBLICATIONS: Information derived from or of value to NASA activities. Publications include final reports of major projects, monographs, data compilations, handbooks, sourcebooks, and special bibliographies.

TECHNOLOGY UTILIZATION PUBLICATIONS: Information on technology used by NASA that may be of particular interest in commercial and other non-aerospace applications. Publications include Tech Briefs, Technology Utilization Reports and Technology Surveys.

Details on the availability of these publications may be obtained from:

SCIENTIFIC AND TECHNICAL INFORMATION OFFICE

NATIONAL AERONAUTICS AND SPACE ADMINISTRATION

Washington, D.C. 20546